

# TEAM YEAGER LAKES



UNIVERSITY OF CALIFORNIA  
SAN DIEGO

2019-2020

AIAA DESIGN, BUILD, FLY  
DESIGN REPORT



Table of contents	Page
<b>1 Executive summary</b>	<b>3</b>
<b>2 Management summary</b>	<b>4</b>
2.1 » Team organization and personnel	4
2.2 » Project timeline	5
<b>3 Conceptual design</b>	<b>6</b>
3.1 » Competition overview and scoring analysis	6
3.2 » Scoring sensitivity analysis	9
3.3 » Translation into design requirements	10
3.4 » Configuration selection	11
3.5 » Final conceptual design	16
<b>4 Preliminary design</b>	<b>17</b>
4.1 » Design and analysis methodology	17
4.2 » Design trade studies	18
4.3 » Lift and drag analyses	23
4.4 » Stability and control analyses	25
4.5 » Mission model	26
4.6 » Expected mission performance	27



Section (§)	Page
<b>5 Detail design</b>	28
5.1 » Final design parameters and specifications	28
5.2 » Structural capabilities	29
5.3 » Sub-system architecture and implementation	31
5.4 » Weight and balance	33
5.5 » Expected flight performance	34
5.6 » Mission modeling	35
5.7 » Drawing package	36
<b>6 Manufacturing plan</b>	37
6.1 » Investigation of manufacturing methodologies	37
6.2 » Selected assembly methods	38
6.3 » Manufacturing timeline	40
<b>7 Testing plan</b>	41
7.1 » Aircraft and sub-system testing plan	41
7.2 » Flight testing	41
<b>8 Performance results</b>	43
8.1 » Component and sub-system performance	43
8.2 » Complete aircraft performance	44
<b>9 Bibliography</b>	48



## 1 Executive summary

This design report, prepared by the DBF team at the University of California, San Diego, extensively describes the design, manufacturing, and testing processes it has adopted to develop an unmanned, remote-controlled bush aircraft capable of chartering peg passengers, towing a banner, and achieving other tasks required to succeed in the 2020 AIAA DBF contest's four missions.

**Design process »** UCSD DBF's conceptual design decisions emphasize the plane's ability to lift heavier payloads, based on the importance of this technical property during the charter and banner missions, and take off in short distances, based on the limitations outlined for the no-load and banner flights (§ 3.1-3.2). These points of emphasis can be resolved by balancing the aircraft's center of gravity and maximizing its thrust-weight ratio. In accordance with these considerations, the team has opted to build a conventional dual-motor plane with tapered trailing-edge wings, Hoerner wing tips, and taildragger landing gear (§ 3.3).

During preliminary design, the team used force analyses and design trades to choose from a multitude of propulsion and aerodynamic configurations (§ 4.1-4.4). In the detail design phase, the team considered the structural makeup of the empennage, fuselage, and wing based on the aircraft's finalized dimensions and balance. This phase also accounts for the design of the plane's sub-systems, such as its loading mechanisms and higher-voltage avionics-- noteworthy as a remedy to a critical issue experienced by the 2018-2019 team's competition aircraft (§ 5.3). These preliminary and detail design decisions form the basis for the provided flight (§ 4.6) and mission (§ 5.7) performance estimations.

**Final capabilities »** Based on data collected during completed test flights (§ 7-8), the 2019-2020 UCSD DBF competition prototype can

- take off within 13 feet at full throttle;
- complete one lap in ss sec. unloaded (ss sec. when loaded);
- endure a flight of 11 min. at cruising speed;
- charter a flight of 18 passengers and their luggage; and
- tow a 50-inch by 10-inch banner.

The remaining sections of this report discuss UCSD DBF's hierarchical structure (§ 2.1), project schedule (§ 2.2), and fabrication plan (§ 6).



## 2 Management summary

### 2.1 Team organization and personnel

UCSD DBF has chosen to follow a hierarchical structure to organize its team members in a way that most effectively assigns responsibility for action items. Two project managers oversee six sub-teams and make final decisions regarding prioritization and team effort. Each sub-team is led by a lead member, who reports on their sub-team's progress to the project managers. [Figure 2.1.1](#) outlines the relationship between members, sub-teams, sub-team leads, project managers, and advisors.

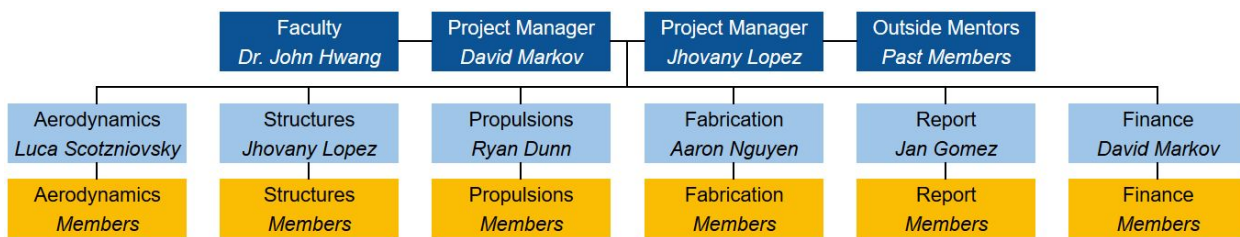


[Figure 2.1.1](#) UCSD DBF's Hierarchical Structure

Each sub-team has a lead member who reports progress in their department to the project managers. The sub-team disciplines that were chosen to organize this year's team include: aerodynamics, structures, propulsions, fabrication, report, and finance. [Figure 2.1.2](#) describes the responsibilities and tasks dedicated to each sub-team. Non-lead members of the team may choose to join any sub-team, but are encouraged to specialize in the operations of a specific sub-team. This structure ensures that these members are sufficiently cross-trained and have enough expertise to succeed outgoing members.

Sub-team	Functions
Aerodynamics	Selects airfoil, sizes wings, and minimizes drag
Structures	Tests and analyzes structures and designs fuselage
Propulsion	Selects motor and propeller, sizes battery, Conducts thrust tests
Controls	Analyzes stability, programs controller, defines flight envelope
Fabrication	Makes components and assembles plane
Report	Writes proposals/reports and communicates competition rules
Finance	Secures funding, networks with industry and handles purchases

[Figure 2.1.2](#) The seven sub-teams and their responsibilities.



## 2.2 Project timeline

UCSD DBF has prepared a project timeline for the 2019-2020 competition, illustrated in [Figure 2.2.1](#), which include the dates of completion for four major objectives. The Gantt chart tracks the progress of the design, analysis, fabrication, and testing of the team's prototype and competition aircraft. The light blue sections represent the weeks each task item is scheduled to be worked on and completed; the team's actual performance is highlighted in yellow.

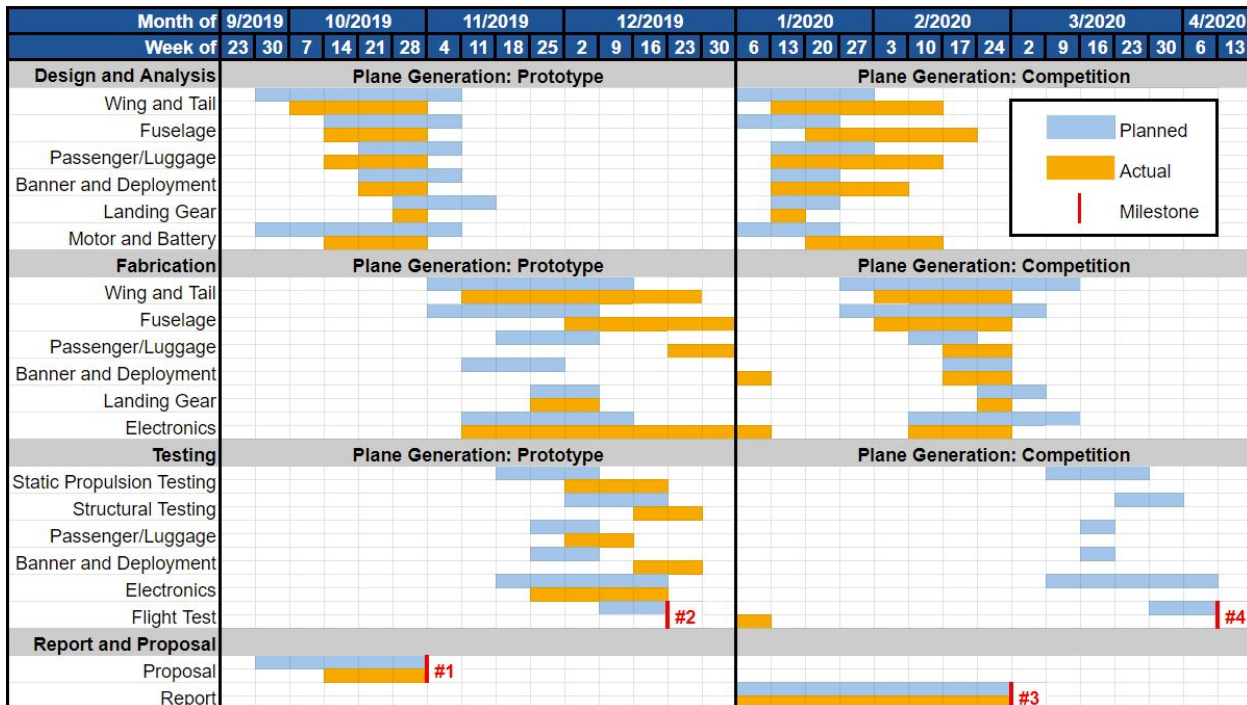


[Figure 2.2.1](#) Project timeline (Gantt chart) for the 2019-2020 competition season.

The red bars on the timeline represent the weeks when a milestone deadline occurs. The team conducts weekly meetings between project managers and sub-team leads to assess the progress of achieving deadlines and milestones. There are four major tasks that the team considers milestones.

Milestone	Deadline	Completion
1. Proposal submission	31 Oct 2019	30 Oct 2019 ✓
2. Prototype plane completion	20 Dec 2019	11 Jan 2020 ✓
3. Report submission	21 Feb 2020	21 Feb 2020 ✓
4. Competition plane completion	10 Apr 2020	...

[Figure 2.2.2](#) Summary of milestone timeline.



## 3 Conceptual design

In the first stage of design, UCSD DBF analyzed competition guidelines, mission requirements, safety regulations, and scoring methodology to establish this season's design requirements. The team then examined several aircraft configurations to develop a realistic prototype, deliverable within the project timeline, to achieve the team's contest goals. The following section discusses this process.

### 3.1 Competition overview and scoring analysis

During the AIAA DBF competition, hosted from 16-19 April 2020 in Wichita, Kansas, teams will complete three flight missions and one ground mission. In conjunction with the score of this design report, the results of these missions comprise the team's total competition score:

$$Sc_{TOT} = Sc_{DR} \times (Sc_{GM} + Sc_{M1} + Sc_{M2} + Sc_{M3})$$

1 Total score.

The team's design motivations are based heavily on the scoring methodology for each mission.

**Ground mission »** Before attempting to fly, teams will participate in a timed demonstration of their aircraft's system and sub-system operations (specifically those pertaining to the charter and banner flight missions). The team's assembly crew member will load passengers, luggage, and the banner onto the aircraft; meanwhile, the team pilot will show that its flight controls and mechanisms are operating normally.

Upon successful completion of the ground mission, teams will become eligible to complete the flight missions. The team will be awarded points based on time of assembly,  $T$ , normalized against the field's fastest:

$$Sc_{GM} = \frac{T_{UCSD}}{T_{fastest}}$$

2 Ground mission score, if team is successful.

**Flight path »** For each flight mission, planes must follow the path that contest guidelines have defined. The route resembles that of a modified oval track, consisting of two 1,000-feet straights connected at its ends by two 180° turns (Figure 3.1.1). The aircraft must

- perform its first turn within 500' of the defined starting line;
- perform a 360° turn each time it flies down the back straight;
- perform a 500' approach on the home straight after completing its final turn; and
- land on the runway in an intact state.

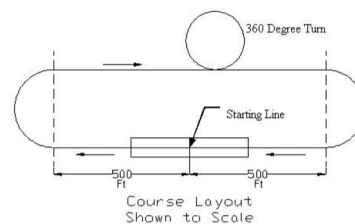


Figure 3.1.1 Flight path.



Henceforth, the term “lap” refers to the completion of one full circuit around this course, finishing in the air directly over the starting line. Throughout this report, the length of a lap is estimated to be 2,500’. Each mission establishes an additional set of requirements that teams must fulfill.

**Mission 1: no-load flight »** After successfully completing the ground mission, teams will demonstrate their unloaded aircraft’s flight capabilities. To complete the first flight mission successfully, planes must abide by the general flight path requirements, take off in a distance shorter within 20 feet of the starting line, and complete three laps within five minutes of takeoff. Teams will simply be rewarded one point upon successful completion; teams are then guaranteed a total score of  $1[\mathbf{Sc}_{\text{DR}}] \leq \mathbf{Sc}_{\text{TOT}} \leq 2[\mathbf{Sc}_{\text{DR}}]$  points.

$$\mathbf{Sc}_{\text{M1}} = 1.0$$

**3** Mission 1 score, if the aircraft completes a successful flight.

**Mission 2: charter flight »** For the second flight mission, teams will simulate a short-haul charter flight. They may elect to load an amount of passengers and luggage parcels,  $nP$ , no greater than the maximum declared during technical inspection. In addition to the general flight path requirements, aircraft must complete three laps within five minutes of takeoff; however, a faster completion time,  $T$ , will improve a team’s score.

This mission does not mandate a minimum takeoff length. If UCSD DBF successfully completes this mission, its score will be determined using a normalized equation:

$$\mathbf{Sc}_{\text{M2}} = 1.0 + \frac{(nP \div T)_{\text{UCSD}}}{(nP \div T)_{\text{highest}}}$$

**4** Mission 2 score, if the aircraft completes a successful flight.

Upon completion of the charter flight, teams are guaranteed a total score of  $2[\mathbf{Sc}_{\text{DR}}] \leq \mathbf{Sc}_{\text{TOT}} \leq 4[\mathbf{Sc}_{\text{DR}}]$  points.

**Mission 3: banner flight »** For the third and final mission, teams will replicate the business of an aerial advertising company by simulating a long-haul banner-towing flight. The deployable banner must fulfill the design restrictions as described by AIAA listed later in this section (banner length,  $BL$ , forms a component of the mission’s scoring methodology). To complete the mission successfully, aircraft must satisfy the aforementioned flight path requirements and take off within 20 feet of the starting line; teams must also deploy their banner while flying the first lap and release it remotely after landing.

Unlike prior missions, teams can fly their aircraft as many laps as possible within a ten-minute window (a greater amount of completed laps,  $nL$ , will benefit a team’s score). If UCSD DBF successfully completes this mission, its score will be determined using a normalized equation:



$$Sc_{M3} = 2.0 + \frac{(nL \times BL)}{(nL \times BL)_{\text{highest}}} UCSD$$

5 Mission 3 score, if the aircraft completes a successful flight.

After completing the flight, teams are assured a total competition score of  $4[Sc_{DR}] \leq Sc_{TOT} \leq 7[Sc_{DR}]$  points.

**Design constraints »** The contest guidelines establish the following requirements regarding the safety, competitive integrity, and overall design of the aircraft:

Category	Constraints
Design	The aircraft cannot exceed a 5' wingspan nor a total, fully-loaded weight of 55 pounds. It cannot utilize a rotary wing nor a lighter than air configuration.
Passengers, luggage, and restraint systems	Passengers, weighing a minimum of 4 ounces, and luggage parcels, weighing a minimum of 1 ounce, must fit the following dimensional requirements: 
Deployable banner	The banner's length can be no less than 10 in.; its aspect ratio, defined as $BL \div BH$ , may not exceed 5. It must be remotely deployed and released, and cannot sustain substantial damage during flight (including due to impact upon release).
Propulsion and power supply	All power for takeoff and flight will be sourced from the aircraft's propulsion system. Teams may use commercially-produced lithium polymer (LiPo), nickel cadmium (NiCad), or nickel metal hydride batteries (NiMH), provided that: <ul style="list-style-type: none"><li>- teams use a single battery type for propulsion; and</li><li>- the safety requirements outlined are fulfilled.</li></ul>

**Figure 3.1.2** Partial list of major design constraints.



### 3.2 Scoring sensitivity analysis

To determine the elements for which the team will optimize its aircraft's design, UCSD DBF conducted a sensitivity analysis of the competition's scoring methodology, as described in § 3.1. This analysis chiefly considers both flight missions whose scores are variable. In the charter and banner flights, four factors influence the team's score. Based on assumptions and general design constraints, the team has derived equations that relate these factors to two parameters, payload weight,  $\mathbf{W}_{\text{added}}$ , and cruise airspeed,  $\mathbf{V}$ .

$$nP = \frac{\mathbf{W}_{\text{added}}}{[4 + 1 \text{ oz}]} -$$

$$BL = \mathbf{W}_{\text{added}} * ([\rho_{\text{banner}}][32.17 \text{ ft/sec}^2][BH * BT])^{-1}$$

$$T = \frac{7500 \text{ ft}}{V}$$

$$nL = \frac{600 \text{ sec} * V}{2500 \text{ ft}}$$

Assuming steady-level flight, these elements are related:

$$\mathbf{W} + \mathbf{W}_{\text{added}} = \frac{1}{2} (\mathbf{C}_L * \mathbf{S} * \rho_{\text{air}} * V^2)$$

6 Passenger-weight relationship for Mission 2.

7 Banner length-weight relationship for Mission 3.  
 $\rho$  is the material density,  
 $BH$  is the banner height, and  
 $BT$  is the banner thickness.

8 Time-airspeed relationship for Mission 2.

9 Laps-airspeed relationship for Mission 3.

10 The lift equation.  
 $\mathbf{W}$  is the aircraft's empty weight,  
 $\mathbf{C}_L$  is the coefficient of lift,  
 $\mathbf{S}$  is the wing area, and  
 $\rho$  is the air density.

By rearranging these equations, the team can establish the constant curves featured in Figure 3.2.1. The blue contours demonstrate how payload score factors affect the base mission score; the yellow contours predict how the added weight impacts the plane's airspeed. If the payload score factors and the aircraft's unloaded (Mission 1) cruise speed are known, the graphs below can project the base mission score. The emboldened curves highlight the team's conceptual design points.

Since the maximum competition base scores cannot be predicted, the team cannot project the normalized scores as discussed in § 3.1.

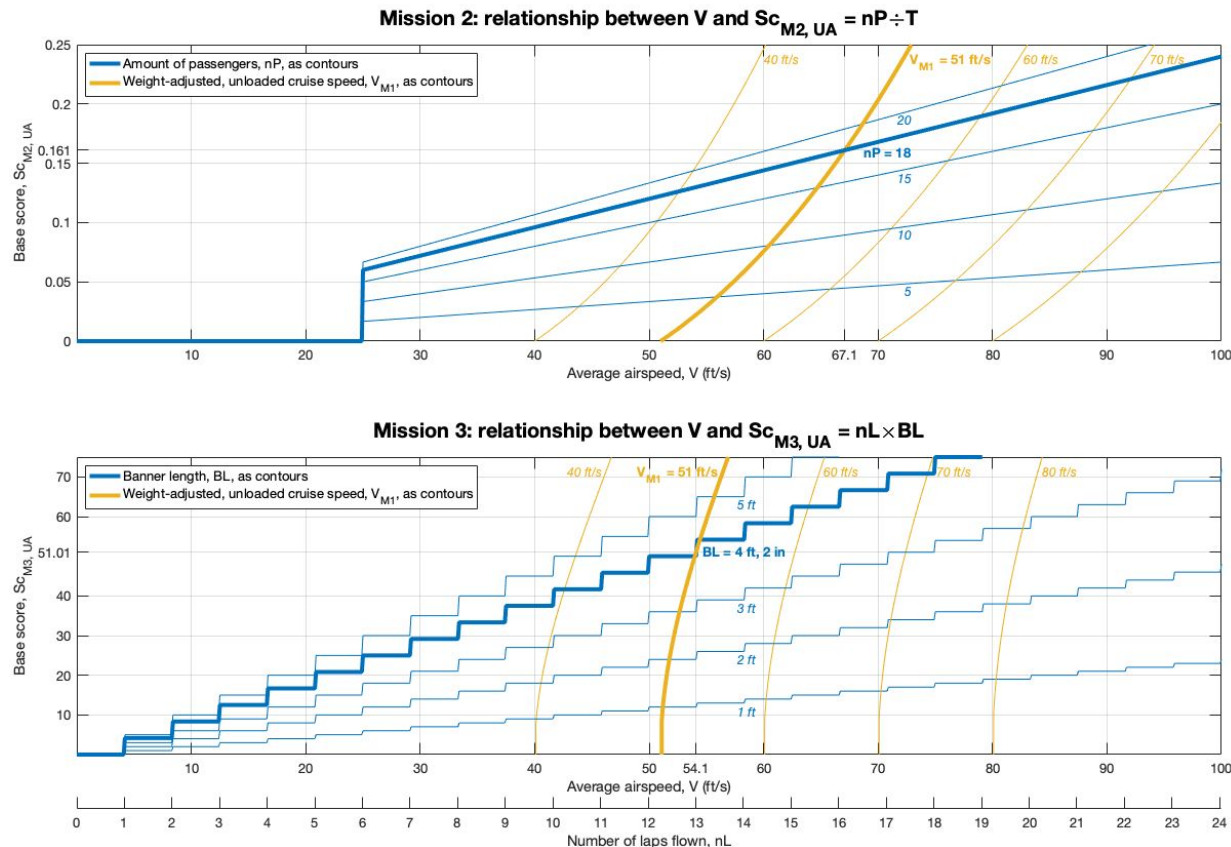


**Figure 3.2.1** The airspeed-base score relationship. Mission 3 analysis assumes that the aircraft flies for the full ten-minute window.

### 3.3 Translation into design requirements

For the range of speeds and loads shown, the yellow contours have steeper slopes than the blue contours, indicating that increasing lift to accommodate heavier loads (i.e. more passengers and longer banners) benefits a team's mission scores more than simply flying faster with the same payload weight. Based on this implication, UCSD DBF will aim to design its aircraft with the ability to carry 18 passengers and a 50-in. banner. To improve the aircraft's ability to carry larger loads and to minimize drag, the team has decided to utilize the 5-foot wingspan-- up to the limit that contest guidelines have established.

Assuming that it can fly at a cruise speed of 51 feet/sec. when unloaded (~7 pounds), the aircraft should be able to sustain a peak cruise speed of at least 67.1 feet/sec. during the charter flight. To do so, the team will optimize the aircraft's propulsion system to maximize its thrust.

Finally, two missions impose a 20-foot limit on takeoff length. To reduce takeoff roll, the team can minimize the aircraft's stall speed, which may also be achieved by increasing the plane's thrust-weight ratio and decreasing its empty vehicle weight.



### 3.4 Configuration selection

With the conclusion that the aircraft must have adequate short takeoff and landing abilities, UCSD DBF considered eight possible design elements that may impact a plane's STOL capability-- aircraft type, wing placement, wing shape, wingtips, empennage, propulsion system, fuselage shape, and landing gear. To help them select an optimal design solution from a large field of configurations, the team has adopted and weighed several figures of merit, listed in [Figure 3.4.1](#).

**Figures of merit »** The team has concluded that it should give more consideration to capabilities that have a greater impact on overall aircraft performance. The team assigned each of the eight figures of merit a weight from 1× (not so important) to 5× (very important); the significance of each figure is based on the design requirements addressed in § 3.3:

Weight	Figure of merit	Figure of merit	Weight
5x	<b>STOL capability</b> Aircraft can take off of, and land on, a minimal runway length	<b>Structural loading</b> Loads are transferred to structural elements, preventing breakage	3x
5x	<b>Aerodynamics</b> Lift is optimized on lifting surfaces; drag is minimized	<b>Flight stability</b> Aircraft retains greater control during maneuvers	2x
4x	<b>Manufacturability</b> Element is easy to manufacture; process is not time-consuming	<b>Mounting</b> Element is attached in a way that doesn't hinder accessibility	2x
3x	<b>Repairability</b> Element is easy to repair, should it be damaged in any capacity	<b>Ground handling</b> Aircraft avoids straying off the runway during takeoff and landing	1x

**Figure 3.4.1** The eight figures of merit in consideration, with their corresponding weight.

**Selection process »** For each figure of merit, each configuration is rated from 1 (low design favorability) to 5 (high design favorability). Their scores are defined as the sum of the products of the figure of merit's weights and ratings. The team has selected the configuration with the highest score.

**Aircraft type »** The main considerations for aircraft configurations were their lift producing and STOL capabilities. While a flying wing scores better in both fields due to their greater wing area and lifting body, it has poor payload capabilities due to the location of the plane's center of gravity. The CG of a flying wing is very close to the nose of the aircraft, making it hard to carry heavier payloads without making the aircraft tail heavy. Thus, the team chose a monoplane because of its ability to carry greater payloads.

Figure of merit	Weight	Monoplane	Flying wing	Lifting body	Biplane
STOL capability	5x	3	4	5	4
Aerodynamics	5x	4	5	5	1
Manufacturability	4x	5	3	1	3
Flight stability	2x	4	1	2	3
Total		63	59	58	43

Figure 3.4.2 Decision matrix of figure of merit for aircraft configuration.

**Wing placement »** When selecting wing placement, the team was most concerned with aerodynamic performance, because the team wanted to maximize the plane's lift and ensure that stall is delayed as much as possible with an increasing angle of attack. Unlike a high or parasol wing, a low and mid wing would have the fuselage in the middle. This heavily impacts the amount of overall lift the wing is capable of producing. In addition, having a mid wing would limit the amount of usable space within the fuselage. A high or parasol wing has the added advantage of having roll stability in gusts by having the center of mass be located below the center of pressure via the keel effect. Between a high and parasol wing, a high wing was determined to be easier to manufacture and mount, making it the preferred choice for a wing placement configuration.

Figure of merit	Weight	High-wing	Parasol	Low-wing	Mid-wing
Aerodynamics	5x	4	5	2	3
Manufacturability	4x	5	2	4	1
Repairability	3x	4	5	4	2
Flight stability	2x	5	4	3	2
Total		62	56	44	29

Figure 3.4.3 Decision matrix of figure of merit for wing placement.

**Wing shape »** The shape of the wing was decided by the stall performances of each wing. While an elliptical wing has the most aerodynamic efficiency at cruising speed, it has poor stall characteristics when compared to a rectangular and trailing edge-tapered wing. The straight leading edge of both wing configurations has the stall starting at the root of the wing and moving outwards instead of at the tip. A tapered trailing edge wing will have the stall forming at the root of the wing while still retaining the low drag characteristics of a traditionally tapered wing.

Figure of merit	Weight	Tapered	Rectangular	Elliptical	Swept
Aerodynamics	5x	4	3	5	4
Manufacturability	4x	4	5	1	3
Repairability	3x	4	4	2	2
Flight stability	2x	5	3	4	2
Total		58	53	43	42

Figure 3.4.4 Decision matrix of figure of merit for wing shape.

**Wingtips »** The team weighed a wingtip's ability to reduce induced drag most heavily when considering different wingtip configurations. Winglets were initially considered as the prominent candidate. However, for the scale and speed of the plane, a winglet would produce more skin friction drag than the induced drag it would reduce. Hoerner wingtips were selected as they offered the highest aerodynamic efficiency while being relatively easy to manufacture.

Figure of merit	Weight	Hoerner	Rounded	Blunt	Winglet
Aerodynamics	5x	5	2	1	3
Manufacturability	4x	3	4	5	2
Repairability	3x	3	5	5	2
Flight stability	2x	3	2	2	4
Total		52	45	44	37

Figure 3.4.5 Decision matrix of figure of merit for the wingtips.

**Propulsion system »** The propulsion systems were scored based on aerodynamic efficiency and thrust output, which a dual tractor setup was deemed best suited for while maximizing the thrust capacity of the plane. In order for a tractor setup to achieve enough static thrust the team wanted, a large propeller and landing gear setup was needed which increases the drag and reduces the aerodynamic efficiency of the plane. A dual tractor setup has the electronic advantage of splitting up the load between two ESCs and motors, reducing the total temperature of the electronics. A dual tractor setup also increases the STOL capabilities of the aircraft by providing constant airflow over the wings from the turning propellers.

Figure of merit	Weight	Dual tractor	Tractor	Pusher	Push-pull
Manufacturability	4x	4	3	2	1
Repairability	3x	3	4	3	2
Flight stability	2x	5	4	3	2
Mounting	2x	3	4	2	1
Total		55	52	42	38

**Figure 3.4.7** Decision matrix of figure of merit for the propulsion system.

**Empennage »** The largest design consideration for the empennage configuration was the turbulent airflow caused by the dual tractor propulsion setup. A T-tail setup raises the horizontal stabilizer above the turbulent air but has a super stall characteristic where at high altitudes, the main wing blocks the T-tail from getting smooth air and induces a superstall after a normal stall. Due to the STOL requirements of Missions 1 and 3, stalls are more likely to happen during flying so a T-tail was not chosen. Although a cruciform tail is not as susceptible to super stalls, this configuration was considered difficult to manufacture and even harder to repair. In turn, the team chose a conventional tail design. To address the turbulent airflow due to the dual tractor propulsion setup, the team will observe pitch stability during the initial test flights and modify if necessary.

Figure of merit	Weight	Conventional	T-tail	Cruciform	V-tail
Aerodynamics	5x	3	4	4	3
Manufacturability	4x	5	4	2	2
Repairability	3x	4	2	2	3
Flight stability	2x	4	5	4	2
Total		55	52	42	38

Figure 3.4.6 Decision matrix of figure of merit for the empennage.

**Fuselage form »** Drag and structural capability are the important factors in deciding the general shape of a fuselage. The presence of landing gear also led to the consideration of how the two elements would be placed and secured with respect to one another. In order to minimize the cross sectional area of the fuselage within the geometric constraint of having a row of more than one passenger, a square fuselage seemed to be most favorable. However, a square fuselage with rounded edges was selected for its superior drag characteristics, as well as having stress concentrations at the corners. An elliptical or circular fuselage would need a greater cross sectional area if a row has more than one passenger, thus increasing drag.

Figure of merit	Weight	Square-ellipse	Circular	Square	Ellipse
Aerodynamics	5x	3	4	2	4
Manufacturability	4x	3	2	4	1
Repairability	3x	4	2	4	3
Structural loading	3x	3	4	2	3
Total		48	46	44	42

Figure 3.4.8 Decision matrix of figure of merit for the fuselage form.

**Landing gear »** The landing gear of the aircraft were selected due to weight and drag considerations. A tricycle gear has the most stability both during take off and landing. Utilizing a tricycle gear also prevents ground looping, an effect where aerodynamic forces cause the advancing wing to rise and the other wingtip to strike the ground. The tail dragger configuration was chosen for being a lightweight landing gear setup that keeps the airplane at an incident angle of attack, which is advantageous for STOL capabilities.

Figure of merit	Weight	Tail dragger	Tricycle	Tip dragger	Tip tricycle
Aerodynamics	5x	4	3	2	1
Repairability	3x	4	3	2	2
Structural loading	3x	3	4	2	2
Ground handling	1x	4	5	3	3
Total		45	41	25	20

Figure 3.4.9 Decision matrix of figure of merit for the landing gear.

### 3.5 Final conceptual design

In accordance with the scoring methodology analysis (§ 3.1-3.3), and after considering many design configurations (§ 3.4), the team will pursue an aircraft design with

- a monoplane aircraft configuration, high-wing, and a conventional empennage;
- a tapered trailing-edge wing, with Hoerner wingtips and a 5-foot wingspan;
- a dual tractor propulsion setup, close to the fuselage;
- a square fuselage with rounded edges; and
- a tail-dragger landing gear.



Figure 3.5.1 Prototype proof of concept.



## 4 Preliminary design

In the preliminary design phase, UCSD DBF conducted analyses of the aircraft's aerodynamic elements, propulsions system, and stability to add to the team's conceptual design point. This section also discusses the methods and models the team utilized to simulate each flight mission.

### 4.1 Design and analysis methodology

Several sub-teams were tasked to conduct analyses relevant to the preliminary design process.

**Aerodynamics »** The aerodynamics sub-team focused on selecting an airfoil that would provide a sufficient lift profile for each mission while operating at a lower Reynolds number for less turbulent flow. The use of different airfoils at the root and tip chord were considered to account for stalling conditions. The aerodynamic coefficients of select airfoils were compared at an angle of attack of zero degrees because it was assumed that aircraft would be cruising at that angle of attack.

The size of the wing was an important parameter considered for efficient flight. To improve the natural wing aerodynamic characteristics, a slight taper was incorporated to increase the wing aspect ratio; this minimal taper allowed for better aerodynamic efficiency while reducing the effects of lift-induced drag and stall capabilities at the wingtips. The ultimate area and tip/root chord length were then determined to minimize the wing weight and match with the desired lift profile for a range of airspeeds.

The aerodynamic coefficients of interest were for lift, drag and moment:  $C_L$ ,  $C_D$ , and  $C_{Mo}$ . These coefficients were found using computational fluid dynamics analysis in XFLR5 and SolidWorks for both the wing and empennage using the dimensions decided when sizing the wing and empennage. A wide range of lift and drag distributions were calculated relative to various cruise speeds.

**Propulsions »** Chief among the design goals for the aircraft's propulsions are to provide enough thrust to overcome drag in-flight, power to perform a short takeoff, and endurance to complete long missions. The team selected

- a battery, based on its large capacity, maximum allowable current, and high voltage;
- a motor, based on its low motor constant ( $K_v$ ), high power ratings, and high efficiency; and
- a propeller, based on its large diameter, high efficiency, and high pitch

to achieve these goals. To simplify the design process, UCSD DBF assumed uniform thrust between the aircraft's two motors and considered only the worst-case scenarios. As all of the stated objectives are factored during both missions, the team will pursue a propulsion system design that maximizes cruise speed for the charter flight and endurance for the banner flight.

**Structures »** The goal of the structures sub-team was to maximize efficiency while maintaining a high margin of safety for all loading conditions. Additionally, empty aircraft weight was minimized without sacrificing strength. Materials chosen for the construction and assembly of the aircraft must resist loads during takeoff, landing, stall, and dive. To meet bare safety requirements, the team decided that the wing would need to withstand load factors in the range of -1.5 and 4.0 ( $-1.5 \leq n \leq 4.0$ ). With a maximum gross aircraft weight of 15 pounds, the team determined that the wings should be designed to be able to resist up to 60 pounds of lift.

## 4.2 Design trade studies

To strike a balance between achieving a high scoring potential and constructing a well-functioning aircraft within a reasonable timeframe, several design trades were made regarding the plane's sub-system architecture.

**Wing aerodynamics »** The team determined that the wing airfoil should have

- optimal lift performance during takeoffs and cruise (i.e. at Reynolds numbers around 500,000);

$$Re = \frac{[c \times \rho_{\text{air}} \times V]}{\mu_{\text{air}}}$$

**11** Reynolds number definition.  
**c** is the chord length, and  
 **$\mu$**  is the dynamic viscosity.

- A thickness of at least 10%, as slimmer airfoils are structurally inadequate;
- a minimal amount of complex geometries, to satisfy the team's manufacturing limitations; and
- optimal coefficient of lift, glide ratio, and stall characteristics.

After examining a short-list of airfoils in XFLR5, primarily considering those with high glide ratios at angles of attack near zero, the team elected to use the E216 airfoil.

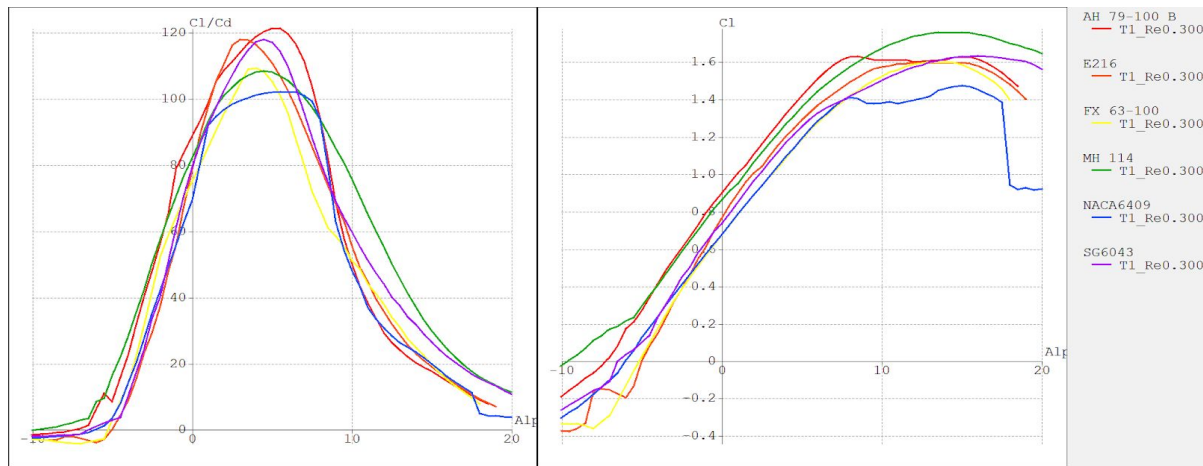


**Figure 4.2.1** Glide ratio (left) and coefficient of lift (right) analyses at  $Re = 500,000$ .

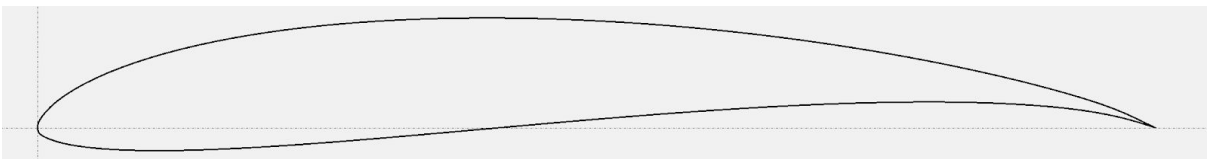


**Figure 4.2.2** The E216 airfoil.

To conduct a sizing analysis, the team considered the weight of the aircraft during each mission. The established conceptual design point suggested that the plane's empty weight is no heavier than 7 pounds, while the sensitivity analysis predicted the plane's gross weight during the charter and banner flights to be 12.6 and 8 pounds, respectively. The team used a safety factor of 1.1 to account for imperfections during the manufacturing process ( $W_{M1} = W = 7.7$  pounds).

The team minimized the plane's induced drag by designing its wing to span the maximum allowable length ( $b = 5$  feet). With these parameters known, the team resolved the wing's dimensions by using equations 12 through 14. These values are documented in [Figure 5.1.1](#).

$$S = \frac{(2 \times W)}{(C_L, \text{takeoff} \times \rho_{\text{air}} \times V_{\text{takeoff}}^2)}$$

**12** Wing area required.

$C_L$  is assumed 1.1, and  
 $V$  is assumed 37 feet/sec.  
 during takeoff.

$$c = \frac{(2 \times W)}{(C_L \times b \times \rho_{\text{air}} \times V^2)}$$

**13** Chord length.

$C_L$  is assumed 0.6, and  
 $V$  is assumed 50 feet/sec.  
 at cruise.

Since it decided to use a tapered wing, the team considered tip and root chord lengths where the mean aerodynamic chord was largely equivalent to the chord length ( $c = 11$  in.) calculated in equation 13.

$$MAC = [0.667][c_{\text{root}}][(1 + \lambda + \lambda^2) / (1 + \lambda)]$$

**14** Mean aerodynamic chord  
 and taper ratio.

$$\lambda = c_{\text{tip}} / c_{\text{root}}$$

**Tail aerodynamics »** For the empennage, the team aimed to pick a symmetric airfoil with a thickness between 9% and 12% and optimal coefficient of lift and stall characteristics; the common NACA 0012 airfoil is a convenient solution for these criteria.

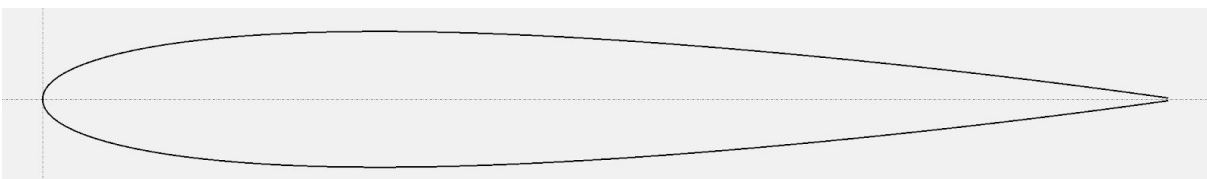


**Figure 4.2.3** The NACA 0012 airfoil.



The team then sized the horizontal and vertical stabilizers and calculated fitting spans from predetermined optimum tail volume coefficients ( $\text{Vol}_h = 1.2$ ,  $\text{Vol}_v = 0.11$ ) and the parameters found during wing sizing. Based on previous aircraft designs, the team chose an elevator and rudder size equal to 28% of the horizontal and vertical tail chord, respectively. These dimensions are also recorded in [Figure 5.1.1](#).

$$\text{Vol}_h = \frac{(L_h \times S_h)}{(S_{\text{wing}} \times \text{MAC})}$$

**15** Horizontal tail volume coefficient equation.

$L_h$  is the distance between the wing and tail.

$$\text{Vol}_v = \frac{(L_v \times S_v)}{(S_{\text{wing}} \times \text{MAC})}$$

**16** Vertical tail volume coefficient equation.

$L_v$  is the level arm.

**Banner sizing »** The team expected the banner to cause a significant portion of the aircraft's drag during the third mission, and thus conducted an experimental analysis to explore its aerodynamic characteristics (as it is difficult to model relationships from a stochastic system, such as the fluttering of a banner). The team assumed that the banner will have an aspect ratio ( $BL \div BH$ ) of 5 and that it will be made mainly from Stretchlon 200 ( $\rho_{\text{banner}} = 2.317 \text{ slugs/feet}^3$ ), an easily-accessible material.

The team organized three test flights to determine the drag caused by the banner; the results of these flights are recorded in [Figure 8.2.3](#). Given that thrust and drag forces are equivalent during steady-level flight and the thrust and throttle percentages are linearly related, the team derived a relationship between  $C_D$  and throttle. Combining several equations, the team derived an optimal banner length ( $BL = 50"$ ).

$$D_B = Th_{22}(V) - [Th \div W][8.8 \text{ lbs.}] - D_{\text{plane}}$$

**17** Available drag.

$$D_B = \frac{1}{2}(C_D \times S \times \rho_{\text{air}} \times V^2)$$

**18** The drag equation.

Since the banner's behavior is largely unpredictable, the team implemented a high safety factor of 1.4.

**Battery selection »** New rules for the 2020 DBF competition allow the usage of lithium polymer batteries (up to a maximum of 100 watt-hours per battery). For its aircraft, the team considered several LiPo and nickel metal hydride batteries. The team elected to use a pack with an optimal power capacity.



Specification	Glacier 6s	Turnigy 5s	Turnigy 6s	LiPos NiMH E5012-B Sub-C Pack
Capacity	4500 mAh	5000 mAh	4000 mAh	5000 mAh
Dimensions	1.8 in. 1.9 in. 5.9 in.	1.6 in. 1.9 in. 5.7 in.	1.6 in. 1.9 in. 5.8 in.	0.9 in. 1.7 in. 5.5 in.
Current	135 A	135 A	135 A	50 A
Maximum power	2997 W	2498 W	2997 W	720 W
Power capacity *	99.9 W-h	92.5 W-h	88.8 W-h	72 W-h
Voltage	22.2 V	18.5 V	22.2 V	14.4 V
Weight	710 g	677 g	650 g	850.5 g

**Figure 4.2.4** Specifications for batteries considered.

\* Contest guidelines limit LiPo batteries to 100 W-h.

In selecting a motor layout, the team primarily considered a setup that could easily fulfill the banner mission's takeoff length requirements. The team used its conservative estimates for the aircraft's mission 3 gross weight ( $W_{M3} = W = 8.8$  pounds) and required takeoff speed ( $V_{takeoff} = 29$  feet/sec.) to determine the required power ( $P_{takeoff} = 358$  W) using equations 19 through 21.

$$V_{takeoff}^2 = 2 * a * L_{takeoff}$$

**19** Fourth applied kinematic equation.

$$a = V' = \frac{[Th(V) - D]}{M}$$

**20** Force balance on an aircraft, assuming level flight.  
 $Th$  is the thrust function.

$$D = \frac{1}{2}(C_D * S * \rho_{air} * V^2)$$

$$P_{takeoff} = Th * V_{takeoff}$$

**21** Power-thrust relationship.

From these calculations the team developed a short-list, primarily favoring motors with a low kV rating to assist the torquing of the aircraft's large propeller. These specifications are:



Specification	Cobra CM-4515/18	Turnigy L3040A-480G	Scorpion HK-3020
kV rating	435	480	1000
Maximum power	1200 W	1000 W	1600 W
Weight	9.63 oz.	6.84 oz.	5.39 oz.

**Figure 4.2.5** Specifications for motors considered.

To accomodate for the large forces and high speeds that the aircraft experiences during the banner flight, the team initially preferred large-diameter, low-pitch propellers; however, the plane's low clearance from the ground and induced airspeed in the propwash became limiting factors to the propeller's size. The team conducted its own test stand experiments and collected data for propellers of various diameters and pitches.

Specification	14" diameter 8.5" pitch	13" diameter 5.5" pitch	14" diameter 5.5" pitch	15" diameter 8.5" pitch
Current	31.5 A	28.44 A	37.89 A	53.52 A
Thrust	116 oz.	103.1 oz.	123.74 oz.	149.6 oz.
Voltage	22.2 V	22.2 V	22.2 V	22.2 V
Manufacturer recommendation	Good size	Good size	Good size	Too large

**Figure 4.2.6** Data for propellers considered.

The team decided that a high-pitch propeller would perform well at high cruise speeds and provide optimal static thrust for the banner flight.

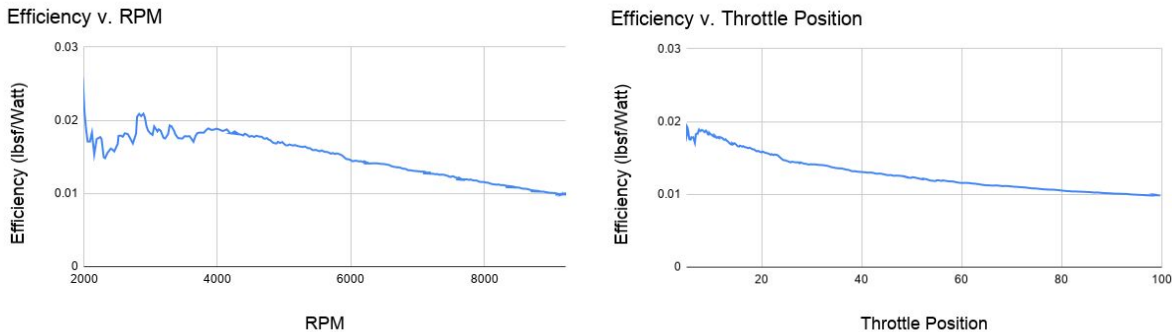


**Figure 4.2.7** Efficiency of the overall propulsion system plotted against RPM and throttle position.

Via momentum analysis on the propeller, the team related maximum thrust as a linear function of velocity [1].



## 22 Thrust-velocity relationship.

For both propellers,

$Th_o$  is assumed 20 lbf, and

$V_o$  is assumed 55 knots.

According to the team's test stand data, this combination of battery, motor, and propeller will allow the aircraft to endure more than 11 minutes of flight.

**Fuselage sizing »** When starting initial sizing of additional components it is important to set design constraints set by necessary and unchanging components. The main structures that must be considered in sizing the fuselage are the carbon fiber spar and the front landing gear. From the sensitivity analysis, it was concluded that 18 passengers and their respective luggage would be the target design parameter. Knowing the diameter of each passenger and luggage, a rough estimate of the minimum size of the fuselage can be found. By seating the passengers in a 3x6 arrangement and the luggage in a 2x3x3 orientation then the minimum length would be 8.75", by 3.375" in width and a 3.56" in height. This is the minimum model, as per competition requirements, the passengers must be separately secured and must contact each other. Due to this constraint, early concepts predicted that the additional structure needed would expand these dimensions to approximately length of 20 inches to house the battery as well. Additionally, the height would be closer to 6 inches to allow it to be attached to the carbon fiber spine as well as provide space for arm access. Similarly, the width had to be widened to approximately 5.5 inches; Not only for the 'seating' structure but to allow hand access to add/remove said structures if needed.

### 4.3 Lift and drag analyses

To better understand its aerodynamic qualities across various flight missions, UCSD DBF analyzed the lift and drag characteristics of the aircraft and each of its parts.

**Lift analysis »** As the team demonstrated during the sensitivity analysis (§ 3.2), it is possible to find a relationship between the aircraft's cruise speed and its weight using the lift equation. The required stall and takeoff speed of the aircraft can be found in a similar manner; however, the plane's angle of attack  $\alpha$  and flaps positions will impact the overall aircraft's coefficient of lift  $C_L$ .

Using XFLR5, the team obtained similar results as shown in [Figure 4.3.1](#) (the calculations completed in § 3.2 do not consider a safety factor, thus creating a slight discrepancy in expected cruise speeds).



Airspeed	$\alpha$	Flaps	Mission 1	Mission 2	Mission 3
Stall	12°	stowed	30.9 ft./sec.	43.2 ft./sec.	33.1 ft./sec.
Takeoff	0°	down	26.6 ft./sec.	37.2 ft./sec.	28.5 ft./sec.
Cruise	0°	stowed	51 ft./sec.	71 ft./sec.	55 ft./sec.

**Figure 4.3.1** Expected stall, takeoff, and cruise airspeeds calculated by XFLR5.

The team then used the program to plot several wing characteristics at each airspeed for its solution:

- coefficient of lift  $C_L$  against angle of attack  $\alpha$  (northeast corner);
- coefficient of lift  $C_L$  against coefficient of drag  $C_D$  (southeast corner);
- $C_L^{1.5} \div C_D$  against angle of attack  $\alpha$  (southwest corner); and
- glide ratio  $C_L \div C_D$  against angle of attack  $\alpha$  (northwest corner).

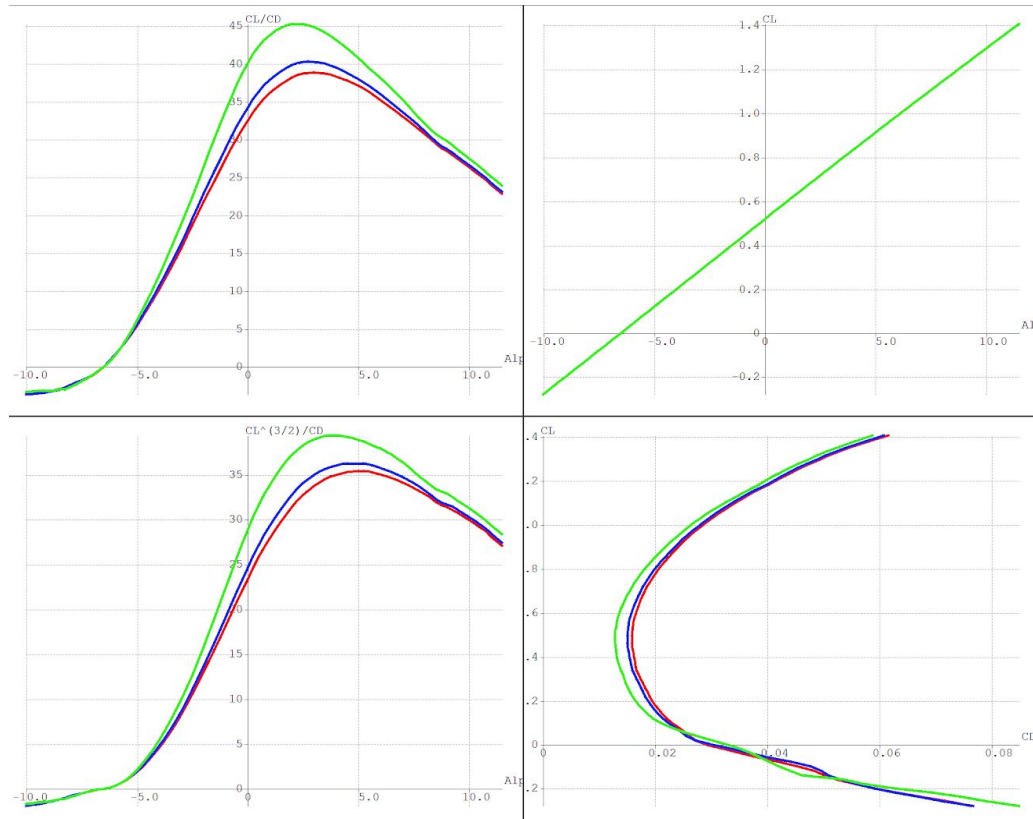


**Figure 4.3.3** Wing characteristics at designated airspeeds.

**Mission 1** is shown in red, **Mission 2** is shown in green, and **Mission 3** is shown in blue.

**Drag analysis »** The team conducted flow simulations in SolidWorks to calculate the total drag of the aircraft at each mission cruise speed. The drag force of the wings, tail, landing gear, and fuselage are listed in Figure 4.3.3.



Component	Mission 1	Mission 2	Mission 3
Banner	--	--	2.5 lb.
Fuselage	0.307 lb.	0.573 lb.	0.385 lb.
Landing gear	0.196 lb.	0.355 lb.	0.197 lb.
Empennage	0.309 lb.	0.904 lb.	0.417 lb.
Wing	0.501 lb.	0.821 lb.	0.498 lb.
<b>Total drag</b>	<b>1.117 lb.</b>	<b>2.298 lb.</b>	<b>4.217 lb.</b>

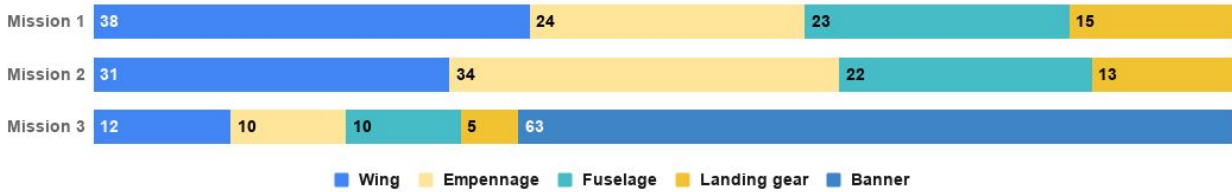


Figure 4.3.3 Percent drag force contribution by each component as a percentage of total drag.

#### 4.4 Stability and control analyses

The team aimed to design an inherently stable aircraft while minimizing the drag. The final plane must be able to fly the competition course effectively while maintaining complete control and stability for the pilot.

**Static margin »** To fulfill one criterion for longitudinal stability, the aircraft's pitching moment coefficient at zero lift  $C_{M_0}$  must be positive; its center of gravity should also be ahead of the position at which the plane is statically neutral. The static margin of the aircraft during each mission quantifies these conditions [2].

$$SM = \frac{(NP - X_{CG})}{MAC}$$

23 Static margin.

The team determined the aircraft's neutral point through XFLR5 ( $NP = 8.27$  in.) and analyzed the position of the aircraft's center of gravity  $X_{CG}$  in SolidWorks. Figure 4.4.1 shows that all static margins are found positive, implying that the aircraft is statically stable for all three flight missions.

Plane characteristic	Mission 1	Mission 2	Mission 3
CG position $X_{CG}$	1.75 in.	4.50 in.	3.25 in.
Static margin	+59.1 %	+34.2 %	+45.5 %

Figure 4.4.1 Center of gravity and static margin.

**Longitudinal stability and trim** » To ensure that the plane is statically stable, the slope of the pitching moment coefficient-angle of attack relationship ( $dC_{M_0}/d\alpha$ ) should be negative when  $C_{M_0} = 0$ . The graphs obtained using XFLR5 in [Figure 4.4.2](#) shows that the team's aircraft satisfies these conditions. The neutral point **NP** is also shown.

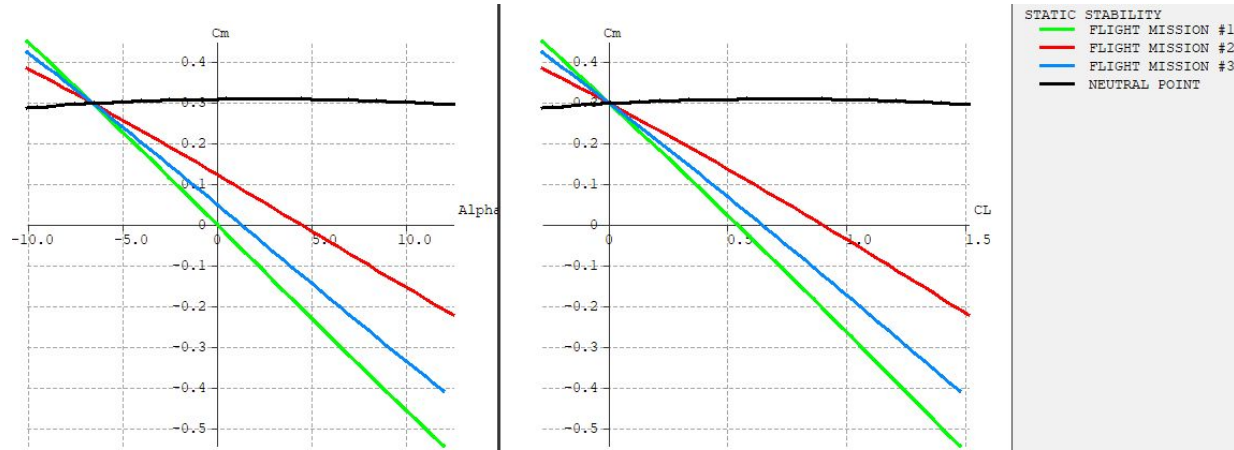


**Figure 4.4.2**  $C_{M_0}$ - $\alpha$  (left) and  $C_{M_0}$ - $C_L$  (right) relationships.

Finally, the overall pitching moment  $C_{M_0}$  acting on a stable aircraft should equal zero; according to Figure 4.4.2, this condition occurs at an angle of attack  $\alpha = 0^\circ, 2.5^\circ, 4.5^\circ$  for Missions 1, 2, and 3, respectively. Because the aircraft will fly at  $\alpha = 0^\circ$  for all missions, the elevator will be individually trimmed for each mission so that  $C_{M_0} = 0$  at this  $\alpha$ .

## 4.5 Mission model

To predict the aircraft's actual in-flight performance, UCSD DBF simulated all three flight missions using a MATLAB-based model.

During level flight, the acceleration is defined using basic equilibrium analysis [3]. To model the motion of the aircraft in non-level flight, the team introduced several parameters, including the plane's vertical flight path angle  $\gamma$  and thrust angle  $\epsilon$ , and expanded upon equation 20.

$$\alpha = V' = [Th(V) \times \cos(\epsilon) - D][m]^{-1} - [32.17 \text{ ft/sec}^2][\sin(\gamma)]$$

**24** Force balance on an aircraft.

If  $\gamma = \epsilon = 0^\circ$ , then equations 20 and 24 are equivalent.

These new parameters must also be modeled, but their governing equations are quite complex. The team used a MATLAB script, developed in previous seasons, that describes the aircraft's dynamics as a large state-space system solvable using an iterative 4<sup>th</sup>-order Runge-Kutta method.



The script outputs flight path (in accordance with the standard route discussed in § 3.1), lap time, and other related data when given relevant vehicle information-- e.g. drag, maximum speed, lift, thrust, and weight. These results are discussed extensively in § 4.6 and § 5.8.

**Model uncertainties »** The team's model assumes that the flight occurs in ideal conditions, and thus carries many inherent uncertainties. These include variations

- in prototype manufacturing, leading to discrepancies from the reported lift, drag, and weight;
- in pilot input, which will inevitably deviate from the idealized flight path;
- in wind and meteorological factors, that are neglected in the model; and
- due to other unpredictable differences between the team's testing site in San Diego and the contest grounds in Wichita.

Thus, the team expects the plane's actual flight performance to vary slightly from the simulated results.

#### 4.6 Expected mission performance

After completing preliminary design and sizing, the team used the mission model to project the aircraft's performance, shown in [Figure 4.6.1](#). Given more accurate lap distance values and takeoff analyses, these values may differ slightly from the sensitivity analysis conducted in § 3.2.

Component	Mission 1	Mission 2	Mission 3
Lap time ( $\pm 5$ sec)	50 sec.	38 sec.	49 sec.
Average airspeed	46 ft./sec.	61 ft./sec.	47 ft./sec.
Maximum airspeed	123 ft./sec.	127 ft./sec.	70 ft./sec.
Minimum airspeed	31 ft./sec.	43 ft./sec.	33 ft./sec.
Projected takeoff distance	4.9 ft.	21.2 ft.	6.6 ft.
Projected unadjusted score	1	0.16	51

**Figure 4.6.1** Expected mission performance.

The team cannot project its final, normalized scores; however, it is evident that the team's design solution can do fairly well across all missions.



## 5 Detail design

In the detail design phase, UCSD DBF optimized the plane's sub-system architecture and finalized design decisions. This section also discusses the plane's structural capabilities and its weight and balance.

### 5.1 Final design parameters and specifications

The aircraft's finalized dimensions, design parameters, and electrical and mechanical specifications are:

Dimension		Overall	Fuselage	Wing	Horizontal stabilizer	Vertical stabilizer
Length	$L$ or $b$	58 in.	36 in.	60 in.	24 in.	12 in.
Width	$W$	60 in.	6 in.	--	--	--
Height	$H$	24 in.	8 in.	--	--	--
Root chord	$c_{root}$	--	--	12 in.	8 in.	8 in.
Tip chord	$c_{tip}$	--	--	10 in.	7 in.	7 in.
Mean chord	MAC	--	--	11.03 in.	7.51 in.	7.51 in.
Area	$S$	--	--	660 in. <sup>2</sup>	180 in. <sup>2</sup>	90 in. <sup>2</sup>
Aspect ratio	$b^2/S$	--	--	5.45	3.2	1.6

Figure 5.1.1 Final aircraft dimensions (values listed as applicable).

Controls	Motor and battery		
Tail servos	KST X08H+	ESC	Frsky Neuron
Stall torque	5.3 kg-cm at 8.4 V	Amp rating	80 A
Servo speed	0.09 sec/60° at 8.4 V	Battery	Glacier 6s
Weight	9.5 g	Number of cells	6 series × 2 parallel
Wing servos	KST X10 Mini	Pack voltage	22.2 V
Stall torque	7.5 kg-cm at 8.4 V	Pack weight	1420 g
Servo speed	0.09 sec/60° at 8.4 V	Motor	Cobra CM-4515/18
Weight	23 g	Kv rating	435

Figure 5.1.2 Electrical and mechanical specifications.

## 5.2 Structural capabilities

To ensure that the aircraft is structurally sound, UCSD DBF has examined how loads, including those resulting from impact with the ground upon landing, compression and tension due to aerodynamic forces and motor thrust, are applied and distributed throughout. The team expects the aircraft to experience critical loading at several locations. From the low order analysis to determine points of concern, two points of interest arose, the wing-boom interface and the motor-spar interface ([Figure 5.2.1](#)).

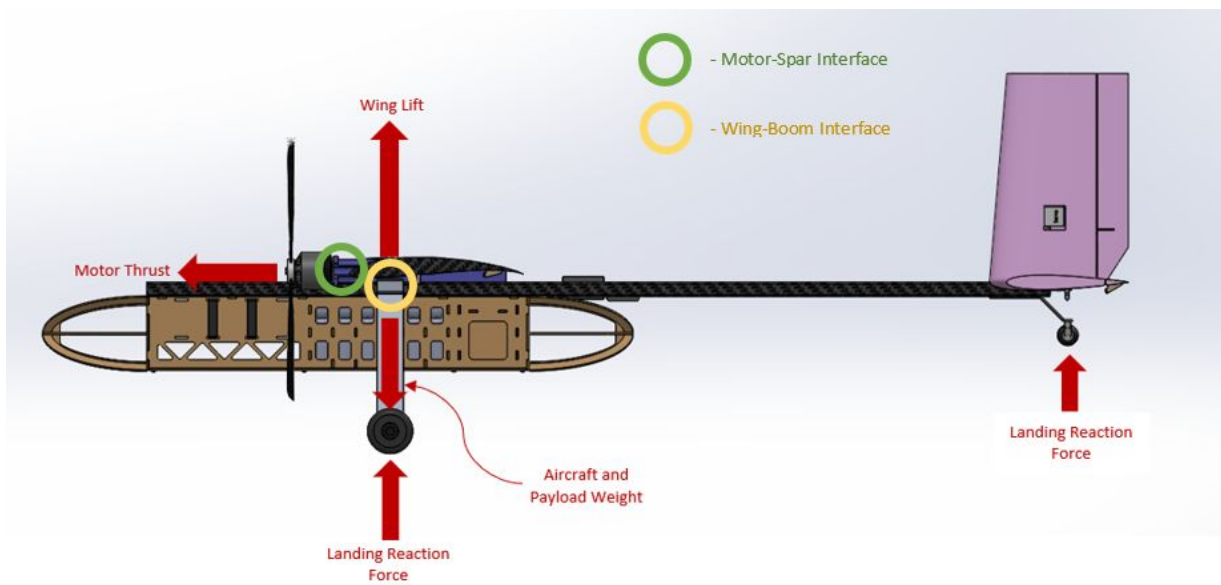


**Figure 5.2.1** Structural load diagram.

The less concerning of the two, the motor-spar interface, was determined through the team's prototype that it will be sufficiently capable of withstanding the thrust force. The wing-boom interface on the other hand raised concerns. The moving of the landing gear was attributed to clearance issues. With the new, finalized fuselage design, it was apparent that the landing gear could not be built into the fuselage. This brought about an exterior landing gear design that would go around the fuselage and use the same mounting bolts as the wing. It would use the same mounting bolts, so as to not introduce additional weak points by drilling into the boom. Assuming that the lift force and landing reaction force act on the boom as point loads at the mounting bolts, the magnitudes of the forces are similar (not order of magnitude different) and that on landing lift drops before contact with ground, it is a sound decision to mount them with the same bolt. Aside from this major structural change, similar capabilities to the prototype should be expected.

**Fuselage »** While the team considered lightweight, strong materials for aircraft components, it preferred a fuselage design that allowed a quick manufacturing process, and thus opted to build a monocoque-like plywood and MonoKote structure. Assembly methods are investigated in further detail in § 6.1 and § 6.2.



To maintain the plane's structural integrity, the team has positioned the fuselage such that its center of gravity  $X_{CG}$  aligns with that of the rest of the aircraft. The fuselage will transfer cargo-induced loads along the aircraft's longitudinal spine-- a hollow, carbon-fiber boom with a cross-sectional area  $A = 0.83 \text{ in.}^2$ ; its ribs will prevent wood members from deflecting.

**Motor mount »** Since it preferred a customized design that can easily conform to the wing airfoil, the team elected to 3D-print both motor mounts. These mounts are printed at an optimal infill percentage to ensure that they can bear the tensile and torsional forces that the team expects it to experience.

**Wing and tail »** With ample experience in composite structure construction, the team believed that the benefits of a foam-core carbon-fiber structure (e.g. its strong and lightweight characteristics) outweighed the cost in assembly time, relative to balsa wood products, and weight, relative to hollow molded structures. The wing core, which retains the wing's distinct shape, is cut from EPS Dow Chemical Bluecore foam ( $\sigma_{compressive} = 60 \text{ psi}$ ); the half-inch diameter carbon-fiber spar strengthens the wing to bear aerodynamic loads. The wing layup is made from Carbonweave ( $\rho = 58 \text{ g/m}^2$ ) carbon-fiber.

The team subsequently decided to build a foam-core empennage without a spar, and will instead apply unidirectional carbon-fibers to provide additional structural support.

**Operating envelope »** Based on the aircraft's aerodynamic and structural limits, the team can determine the conditions at which the plane can be flown safely. It is designed to bear a maximum load factor  $n_p$  of 4 and a minimum load factor  $n_n$  of -1.5 at its fully-loaded design weight. The aircraft's stall, cruise, and dive speeds are estimated based on values the team obtained in § 4.3.

In addition, the team considered the effects of horizontal gusts on the plane. Head and tail gusts create loading that changes the aircraft's operating envelope [4]. The team considered a maximum gust speed of 36.6 feet/sec.

The **V-n** diagrams shown in [Figure 5.2.3](#) represent the plane's operating envelope graphically.

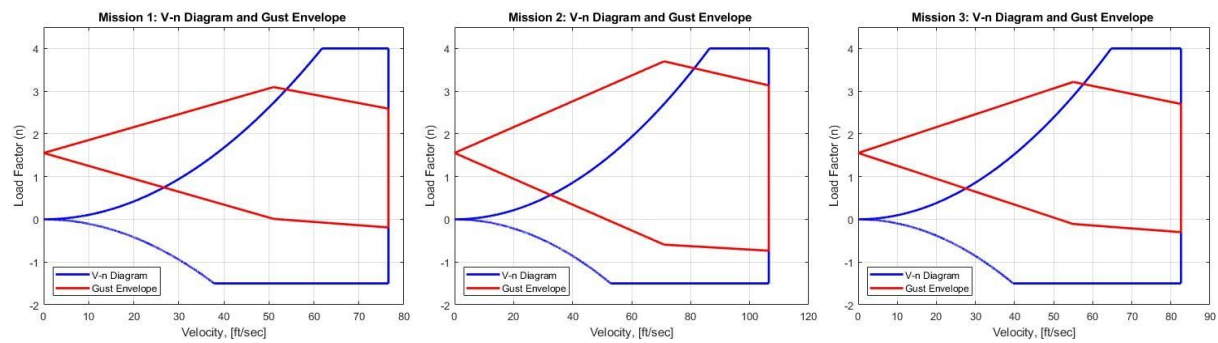


**Figure 5.2.1** V-n diagrams and gust envelopes for each mission.

### 5.3 Sub-system architecture and implementation

The team finalized the aircraft design process by investigating the mechanics of its sub-systems and the implementation of its avionic system.

**Passenger and luggage restraint systems »** The passenger restraint system consists of a plywood compartment and an internal plywood grid-- this prevents passengers from touching one another, orients them in a vertical position, and locates them within the same X-Y plane (as defined by the contest design constraints). Passengers are inserted into the compartment from the bottom of the aircraft, and are supported in place by 3 mm aluminum rods that pass through holes in the grid structure. One-and-a-half millimeter holes are drilled through both ends of the rods, allowing us to insert R-Clips which prevent the rod from shifting in flight.

The luggage compartment is located directly behind the passengers. This restraint system is much simpler, as the weight of the luggage is significantly less than the passengers. The monocoque bottom plate serves an aerodynamic purpose and does not provide any structural support for the batteries or passengers. With this in mind, the plate was designed to have relief cuts for weight savings beneath the batteries and passengers. The bottom plate was left solid beneath the luggage and is firmly mounted to the bottom of the fuselage, restraining the luggage. Half-inch cube wooden blocks with a hole drilled through and 6-32 blind nuts pressed into the back of them, are adhered to the inside structure at multiple points along the fuselage. The hardpoints allow us to securely fasten the bottom plate to the fuselage using 0.75-in. 6-32 screws.

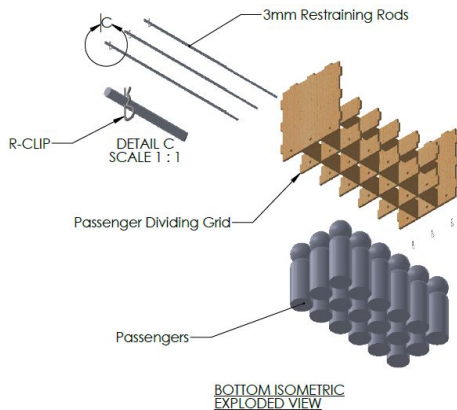


**Figure 5.3.1** Passenger restraint system

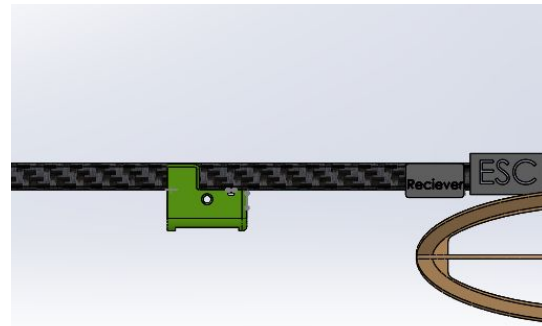


**Figure 5.3.2** Banner deployment and release mechanism

**Banner deployment and release mechanism »** A single servo 3D-printed mechanism was designed and manufactured for its simplicity and light weight. The servo is able to both deploy the banner and release the banner through a two-way pushrod setup. When the servo arm is rotated in one direction, the first string is released and the banner is deployed. When the servo arm is rotated in the opposite direction, the second string which holds the tow line for the banner is released.

**Avionics »** The Frsky Neuron 80 ESCs were chosen to drive the motors due to their built in current sensor, voltage sensor, motor RPM, power consumption and ESC temperature sensor. The Neuron is also a 32 bit ESC which means smoother motor cogging and faster throttle response time.

The team selected the Frsky X9D+ transmitter and S8R receiver because of its ability to send in-flight telemetry data from the Frsky ESC, receiver, and external sensors to the transmitter live during flight. The X9D+ displays live data and writes to a memory card. ESC temperature, RPM, current draw, and voltage can be read when using it in conjunction with a Frsky 80A Neuron 32-bit ESC through the special S.Port telemetry port. A Frsky pitot-tube is daisy-chained into the S.Port to write airspeed readings for testing.

Due to a receiver brownout during the 2019 competition, the aircraft's avionics are running on a higher 8.4 V, reducing the chance of a brownout and increasing response time and torque from the onboard servos. KST X08N V5s were chosen for the tail servos due to their wide voltage range, light weight, and aluminum outer construction. Sub-Micro servos are usually not preferred for tail servos-- but at 8.4 V, the KST X08Ns produce 39 oz.-in. of torque. For the wing servos, KST X10-710s were chosen because they provide 104.16 oz.-in. of torque at 8.4 V, are shorter than traditional wing servos, and weigh 23 g each.



## 5.4 Weight and balance

Figure 5.4.1 includes the plane's component weights and positions from the motor firewalls (**X**-distance) and above and below the thrust line (**Z**-direction), along with the resultant weight and center of gravity positions for all configurations. Since the aircraft is symmetrical around the centerline, the distance along the **Y**-direction is ignored.

Component	Case	Weight	X-distance	Z-distance
Batteries (x2)	All missions	46.00 oz.	-6 in.	2 in.
Electronic speed controls (x2)	All missions	4.02 oz.	16 in.	1 in.
Fuselage	All missions	10.11 oz.	3 in.	2 in.
Landing gear	All missions	3.41 oz.	2 in.	4 in.
Motors	All missions	20.67 oz.	0 in.	0 in.
Receiver	All missions	0.46 oz.	15 in.	1 in.
Tail	All missions	3.52 oz.	38 in.	1 in.
Wing	All missions	17.63 oz.	2 in.	3 in.
Luggage block (x18)	Mission 2	18.00 oz.	9 in.	2 in.
Passengers (x18)	Mission 2	72.00 oz.	3 in.	2 in.
Banner	Mission 3	15.66 oz.	29 in.	3 in.
Banner release mechanism	Mission 3	2.25 oz.	24 in.	2 in.
<b>Mission 1 Total</b>		<b>108.07 oz.</b>	<b>3.25 in.</b>	<b>1.75 in.</b>
<b>Mission 2 Total</b>		<b>198.07 oz.</b>	<b>4.10 in.</b>	<b>2.35 in.</b>
<b>Mission 3 Total</b>		<b>123.73 oz.</b>	<b>3.40 in.</b>	<b>2.05 in.</b>

Figure 5.4.1 Weight and balance. Distances in the **X**-direction are measured from the motor mounts.  
Distances in the **Z**-direction are measured from the thrust line.



## 5.5 Expected flight performance

The team was able to identify relevant flight performance parameters for various angles of attack through the use of CFD analysis. The test cases analyzed were performed at angles of attack of 0, 4, 8, and 12 degrees. These test cases represented the expected parameters for steady-level flight, takeoff, climb, and landing. Excepted flight performance parameters are recorded in [Figures 5.5.1](#), [5.5.2](#), and [5.5.3](#).

Angle of attack $\alpha$	$C_L$	$C_D$	Turn rate	Weight
0°	0.540	0.035	140°/sec.	7.7 lb.
4°	0.862	0.058	176°/sec.	7.7 lb.
8°	1.175	0.096	206°/sec.	7.7 lb.
12°	1.476	0.154	231°/sec.	7.7 lb.

**Figure 5.5.1** Expected flight performance for Mission 1.

Angle of attack $\alpha$	$C_L$	$C_D$	Turn rate	Weight
0°	0.540	0.031	100°/sec.	15.0 lb.
4°	0.862	0.056	126°/sec.	15.0 lb.
8°	1.175	0.094	147°/sec.	15.0 lb.
12°	1.476	0.150	215°/sec.	15.0 lb.

**Figure 5.5.2** Expected flight performance for Mission 2.

Angle of attack $\alpha$	$C_L$	$C_D$	Turn rate	Weight
0°	0.540	0.186	130°/sec.	8.8 lb.
4°	0.862	0.206	165°/sec.	8.8 lb.
8°	1.175	0.247	193°/sec.	8.8 lb.
12°	1.476	0.304	165°/sec.	8.8 lb.

**Figure 5.5.3** Expected flight performance for Mission 3.

## 5.6 Mission modeling

Using aircraft parameters and mission analysis code, the team was able to calculate estimated performance for each of the missions. This analysis allowed the team to identify critical stages of flight and identify corresponding deficiencies. In particular, the team considered: aircraft loading, airspeed, turn rate, bank angle, climb angle, and altitude. Flight path is plotted for Missions 2 and 3 in [Figure 5.6.3](#). Airspeed for one lap is shown by [Figure 5.6.1](#) and g-loading is shown in [Figure 5.6.2](#), the markers represent the start of the specified event. From these figures it was determined that at no point in the missions does the aircraft stall, or exceed the maximum acceleration of 2.5g, during turning and level flight. Additional parameters are included in Table 5.7.

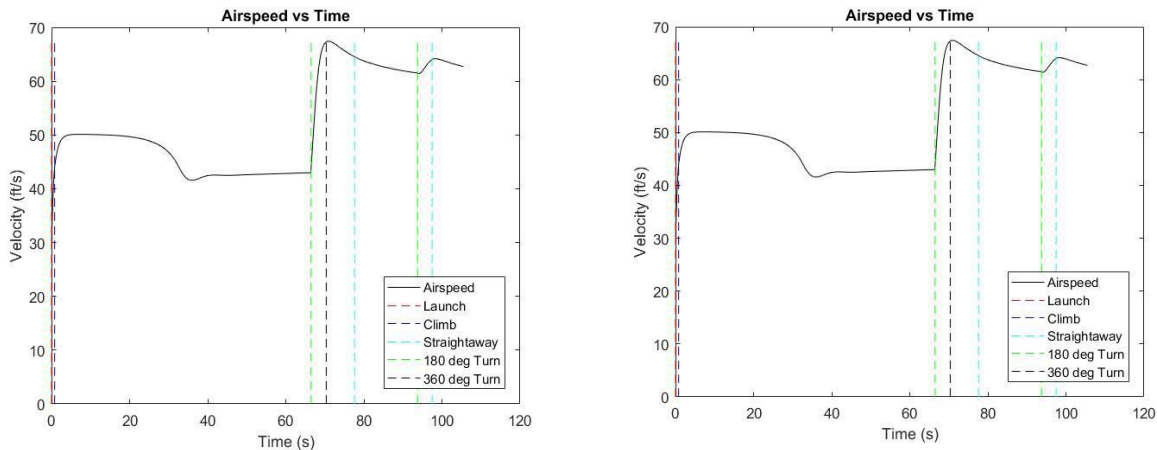


**Figure 5.6.1** Airspeed-time relationship for Mission 2 (left) and 3 (right), according to MATLAB simulation.

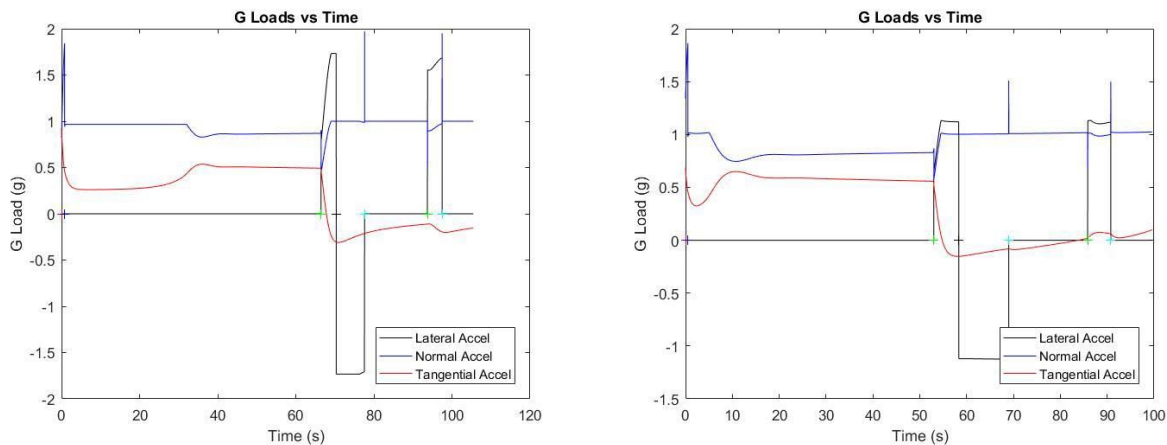


**Figure 5.6.2** Load factor-time relationship for Mission 2 (left) and 3 (right), according to MATLAB simulation.

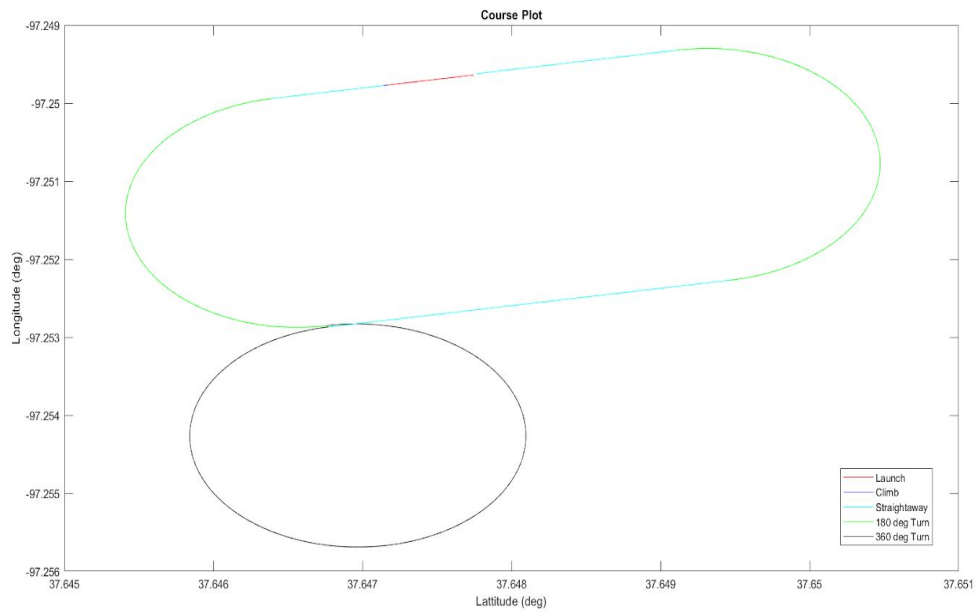


**Figure 5.6.3** Latitude-longitude relationship (map of the flight course in Wichita, Kansas).

### 5.7 Drawing package

The next pages contain the drawing package for the UCSD 2020 DBF competition aircraft. In order, they are: a three-view drawing, an exploded view, a fuselage exploded view, a luggage compartment exploded view, and a passenger compartment exploded view.

4

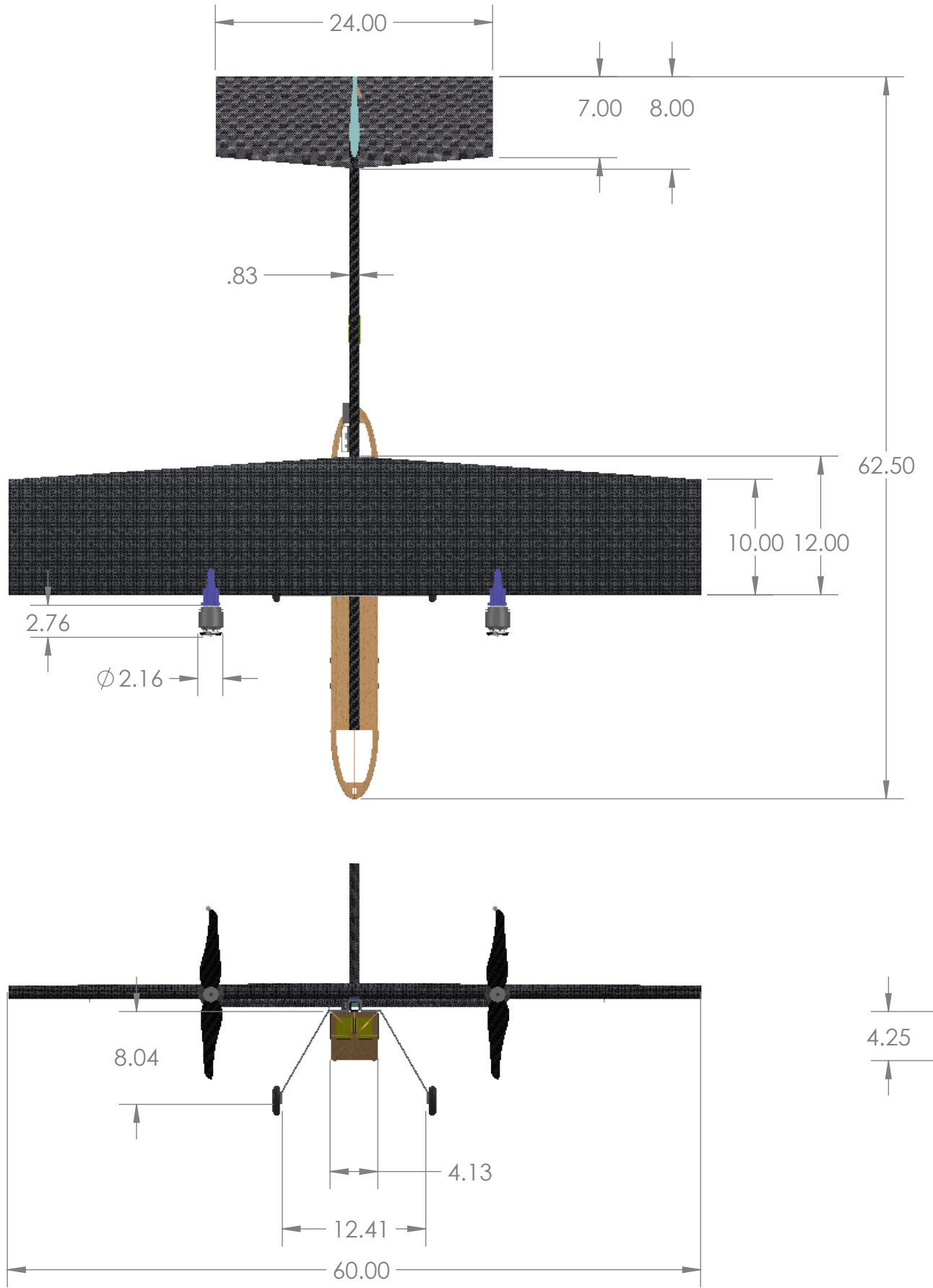
3

2

1

B

B



3

2

1

2

1

3

2

1

2

1

3

2

1

2

1

3

2

1

2

1

3

2

1

2

1

3

2

1

2

1

3

2

1

2

1

3

2

1

2

1

3

2

1

2

1

3

2

1

2

1

3

2

1

2

1

3

2

1

2

1

3

2

1

2

1

3

2

1

2

1

3

2

1

2

1

3

2

1

2

1

3

2

1

2

1

3

2

1

2

1

3

2

1

2

1

3

2

1

2

1

3

2

1

2

1

3

2

1

2

1

3

2

1

2

1

3

2

1

2

1

3

2

1

2

1

3

2

1

2

1

3

2

1

2

1

3

2

1

2

1

3

2

1

2

1

3

2

1

2

1

3

2

1

2

1

3

2

1

2

1

3

2

1

2

1

3

2

1

2

1

3

2

1

2

1

3

2

1

2

1

3

2

1

2

1

3

2

1

2

1

3

2

1

2

1

3

2

1

2

1

3

2

1

2

1

3

2

1

2

1

3

2

1

2

1

3

2

1

2

1

3

2

1

2

1

3

2

1

2

1

3

2

1

2

1

3

2

1

2

1

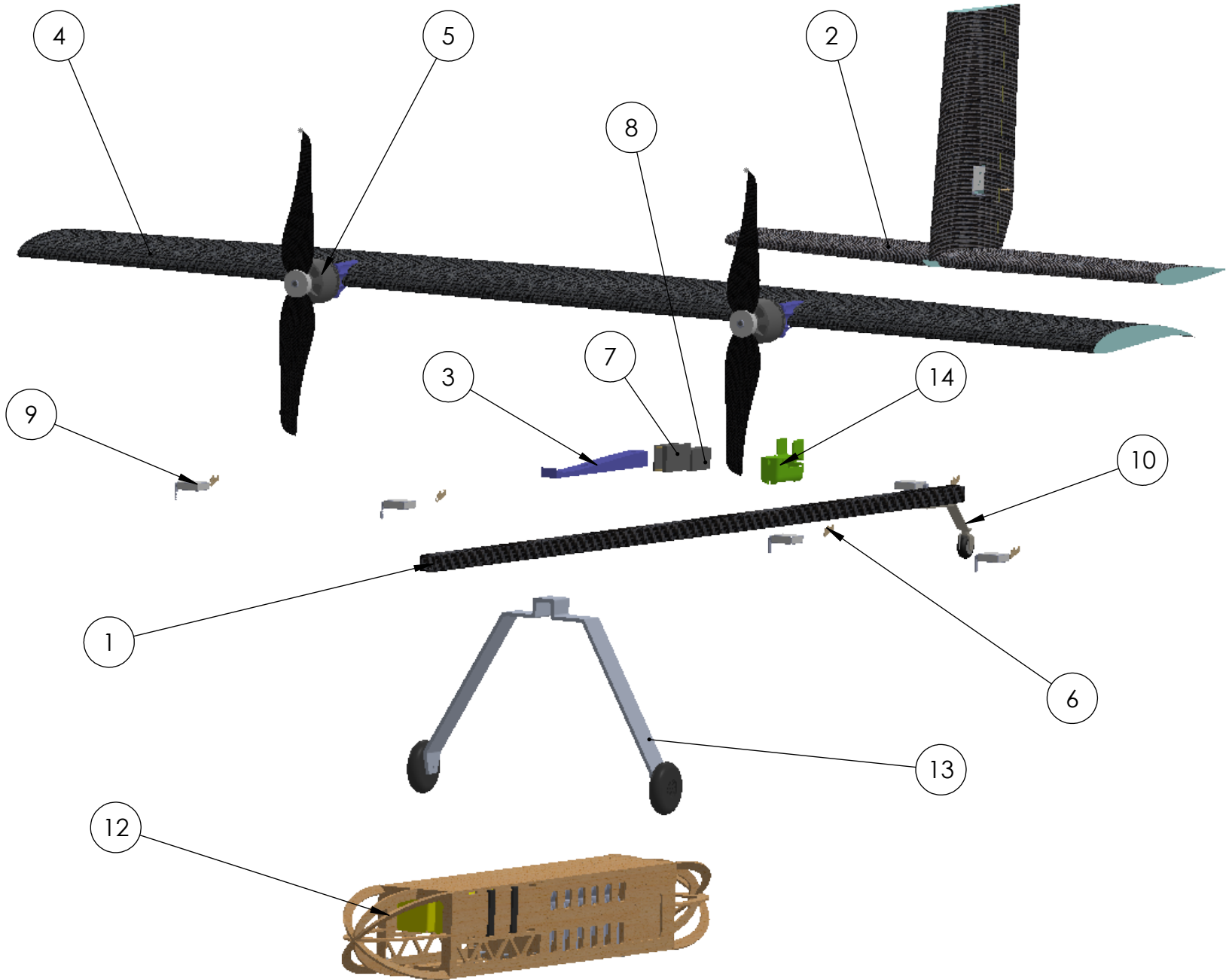
4

3

2

1

ITEM NO.	PART NUMBER	QTY.
1	Carbon Fiber Boom	1
2	Empennage	1
3	Wing Base	1
4	Wing	1
5	Motor Assembly	2
6	Servo Horn	6
7	ESC	1
8	Receiver	1
9	Servo	6
10	Rear Landing Gear	1
12	Fuselage	1
13	Landing Gear	1
14	Banner Release Mechanism	1



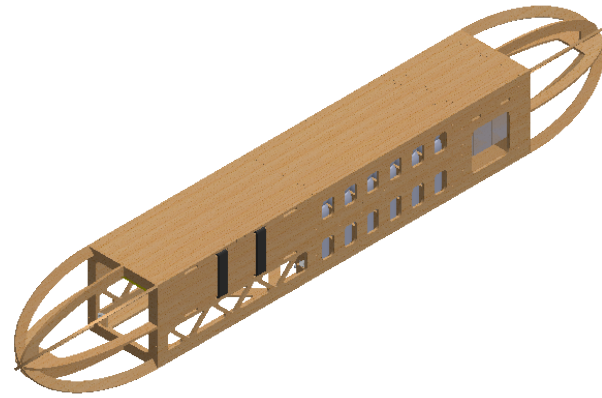
University of California San Diego

TITLE:  
**Exploded View**

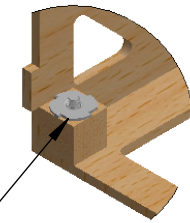
SIZE	DWG. NO.	REV
<b>B</b>		
SCALE: 1:16	WEIGHT:	SHEET 2 OF 2

2

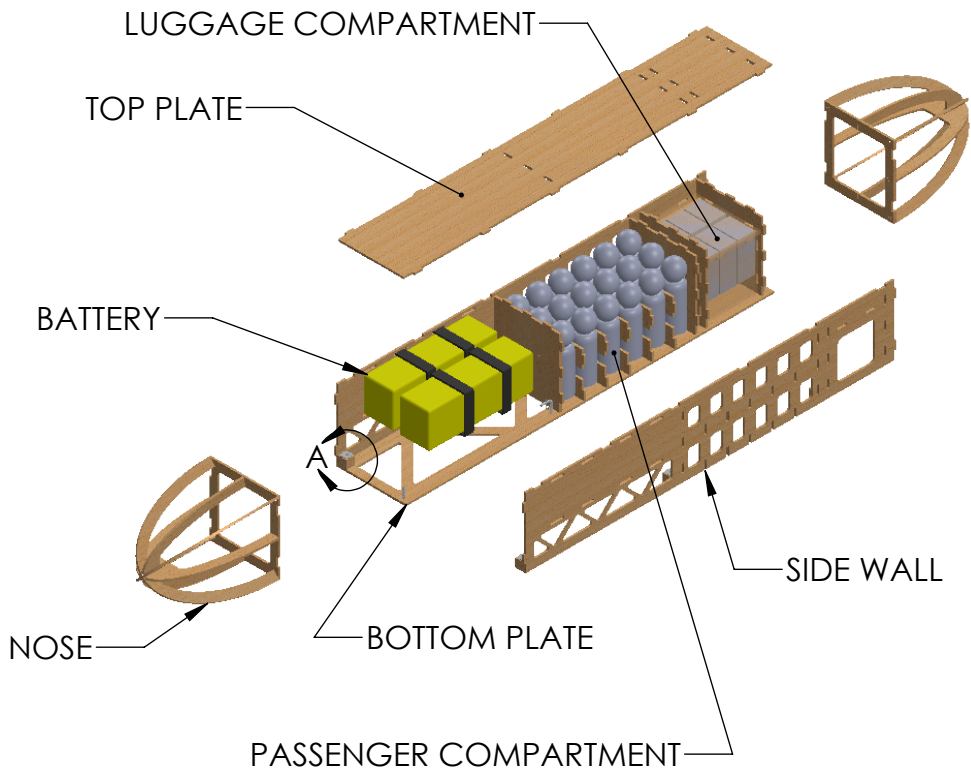
1

ISOMETRIC VIEW

0.5X0.5X0.5 WOOD BLOCK  
WITH 6-32 THREADED BLIND NUT  
FOR SECURING BOTTOM PLATE

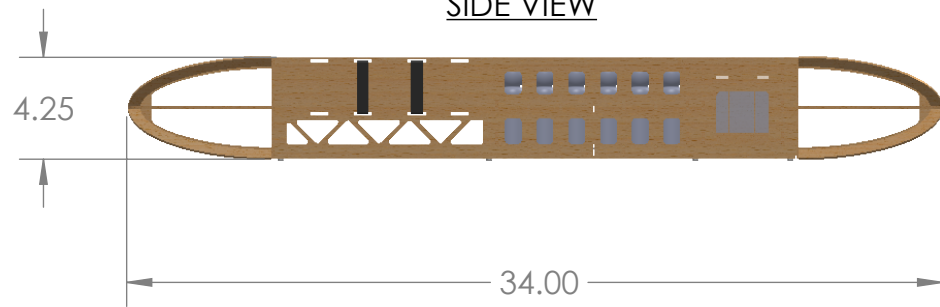


DETAIL A  
SCALE 1 : 2

EXPLODED ISOMETRIC VIEW

B

A

SIDE VIEW

TITLE: Fuselage

DIMENSIONS: INCHES

SIZE	DWG. NO.	REV
A		

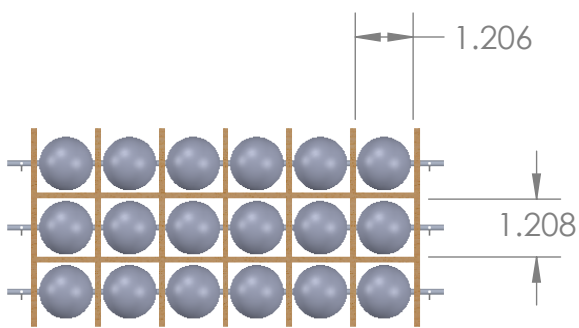
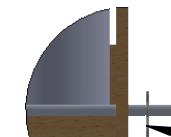
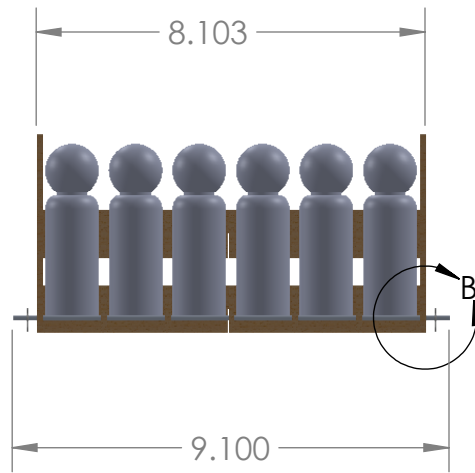
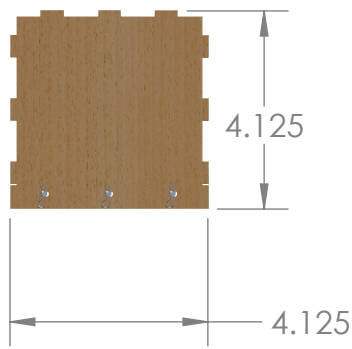
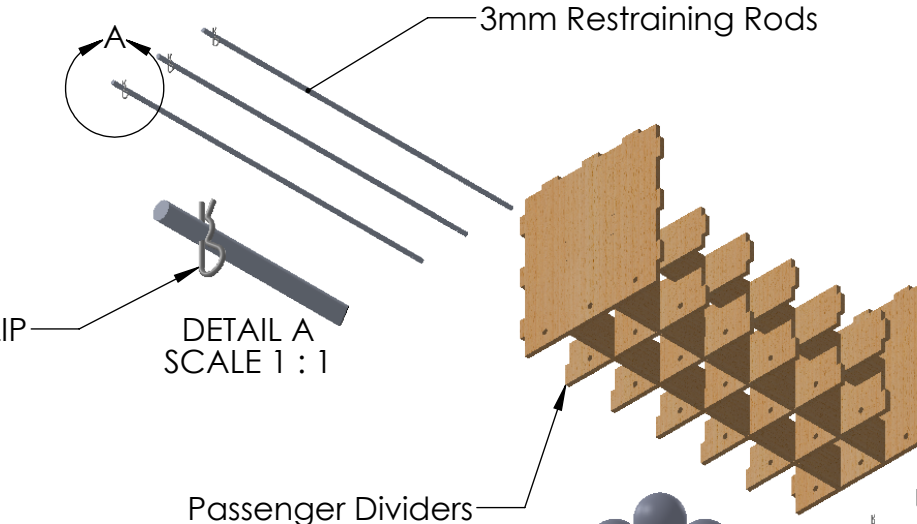
SCALE: 1:10 WEIGHT: SHEET 1 OF 3

2

1

2

1

TOP VIEWRIGHT VIEWDETAIL B  
SCALE 1 : 2FRONT VIEWR-CLIP ON BOTH SIDES OF  
RESTRAINING RODBOTTOM ISOMETRIC  
EXPLODED VIEW

TITLE:  
**Passenger\_Compartment**

DIMENSIONS: INCHES

SIZE	DWG. NO.	REV
<b>A</b>		

SCALE: 1:8 WEIGHT: SHEET 2 OF 3

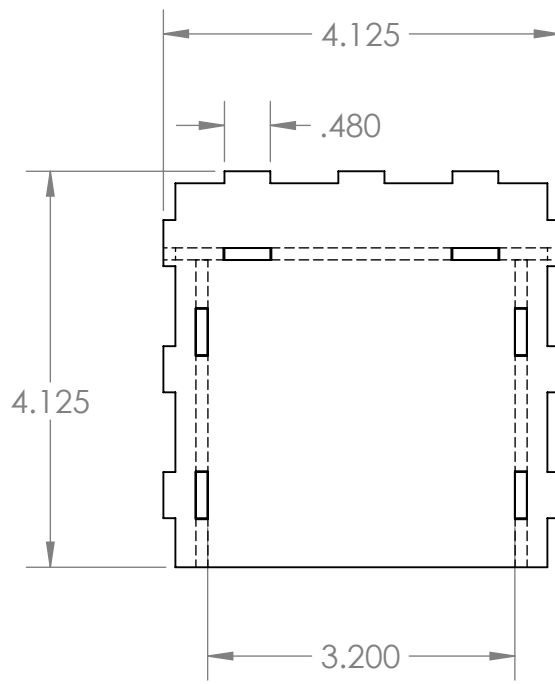
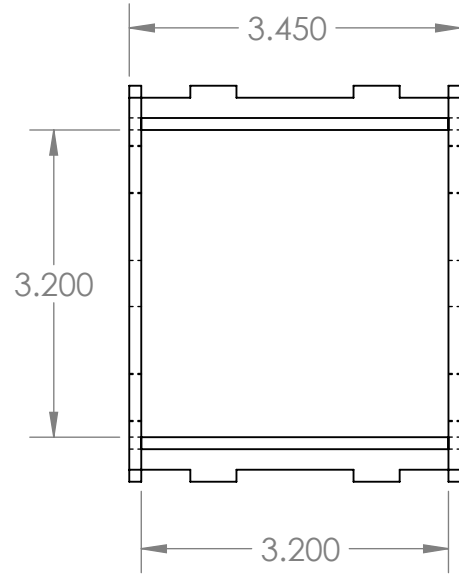
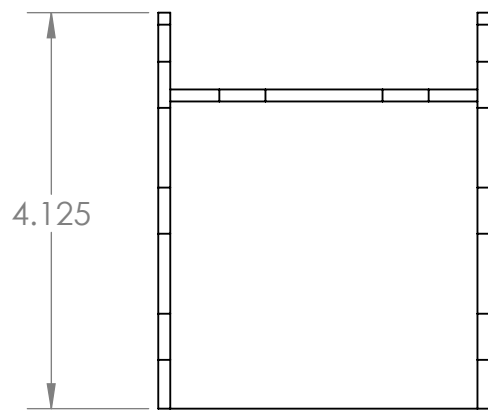
2

1

2

1

B



B

A

TITLE: Luggage\_Compartment

DIMENSIONS: INCHES

SIZE	DWG. NO.	REV
A		

SCALE: 1:2 WEIGHT: SHEET 3 OF 3

NOTE: LUGGAGE IS PLACED INTO THE 3.2X3.2X3.2 COMPARTMENT  
FROM THE BOTTOM AND SECURED IN PLACE BY THE FUSELAGE BOTTOM PLATE.



## 6 Manufacturing plan

After completing principal design, UCSD DBF considered several different construction methods to build a high-performance, highly-reliable aircraft in time for competition.

### 6.1 Investigation of manufacturing methodologies

In the interest of adopting a method of assembly that can fulfill its design criteria and that can be carried out in a reasonably timely and monetarily cheap manner, the team considered the advantages and disadvantages of each process:

Process	Description
3D printing	While not as strong as injection molded parts, 3D printing is inexpensive and parts can be quickly made. It is most effective at creating complex mechanisms when weight is insignificant.
Balsa wood	Balsa wood construction is the cheapest and most expedient method of building an airplane; however, it requires an involved digital process to design and build its complex ribbed structure.
Carbon fiber composites	Carbon fiber is a very stiff and strong material. But construction is quite time-consuming and expensive, and it tends to block radio-frequency signals.
Fiberglass composites	Fiberglass is less stiff and less strong than carbon fiber, but does not block radio signals. It shrinks and distorts when cut, making it harder to manufacture.
Foam-core structures	Foam is a very light material that can generate shapes (e.g. fuselages and wings). When used with composite materials, it acts as a spacer and increases overall strength.
Hollow molded structures	A mold can be created using various materials (e.g. liquid mold material, fiberglass, or plastic) and used with composites to make a hollow molded final product.

**Figure 6.1.2** Manufacturing methods in consideration.



## 6.2 Selected assembly methods

The team combined general processes as outlined in [Figure 6.1.2](#) to develop manufacturing methods specific to an individual component, and compared these part-specific methods.

**Fuselage »** The team considered several fuselage assembly methods:

- a wood truss and MonoKote based process, in which the team uses a laser cutter to cut plywood and balsa wood formers, and covers the structure in MonoKote;
- a hollow bladder molded process, in which the team makes a positive mold from high-density foam and fiberglass and a negative mold from fiberglass, and inserts a balloon inside this structure to apply pressure on the composite material;
- a carbon-fiber based process, in which the team makes a positive mold from foam, lays carbon-fiber over the mold, and cures the structure.

While composite-based constructions provide slight weight reductions and strength improvements, the relatively quick manufacturability of a wood truss and MonoKote fuselage allows the team to prototype multiple fuselage designs.

**Wing »** The team investigated several wing manufacturing processes, including:

- a foam-core composite process, in which the team uses a hot-wire computer numerical control cutter to cut airfoils from high-density foam, epoxies a carbon-fiber spar in the center, and covers the structure with composite material;
- a hollow composite process, in which the team makes a foam-core composite wing and removes the foam, making the wing more lightweight; or
- a wood-rib construction process, in which the team uses a laser cutter to cut airfoil sections from balsa wood, connects each section with thin spars, and covers the structure with film.

Of the processes considered, foam-core composite wings amount to the strongest and lightest. Since the team has ample experience in composite construction, it felt that these benefits far outweighed the cost in assembly time relative to balsa wood construction. The material composition of these components are discussed in further detail in § 5.2.

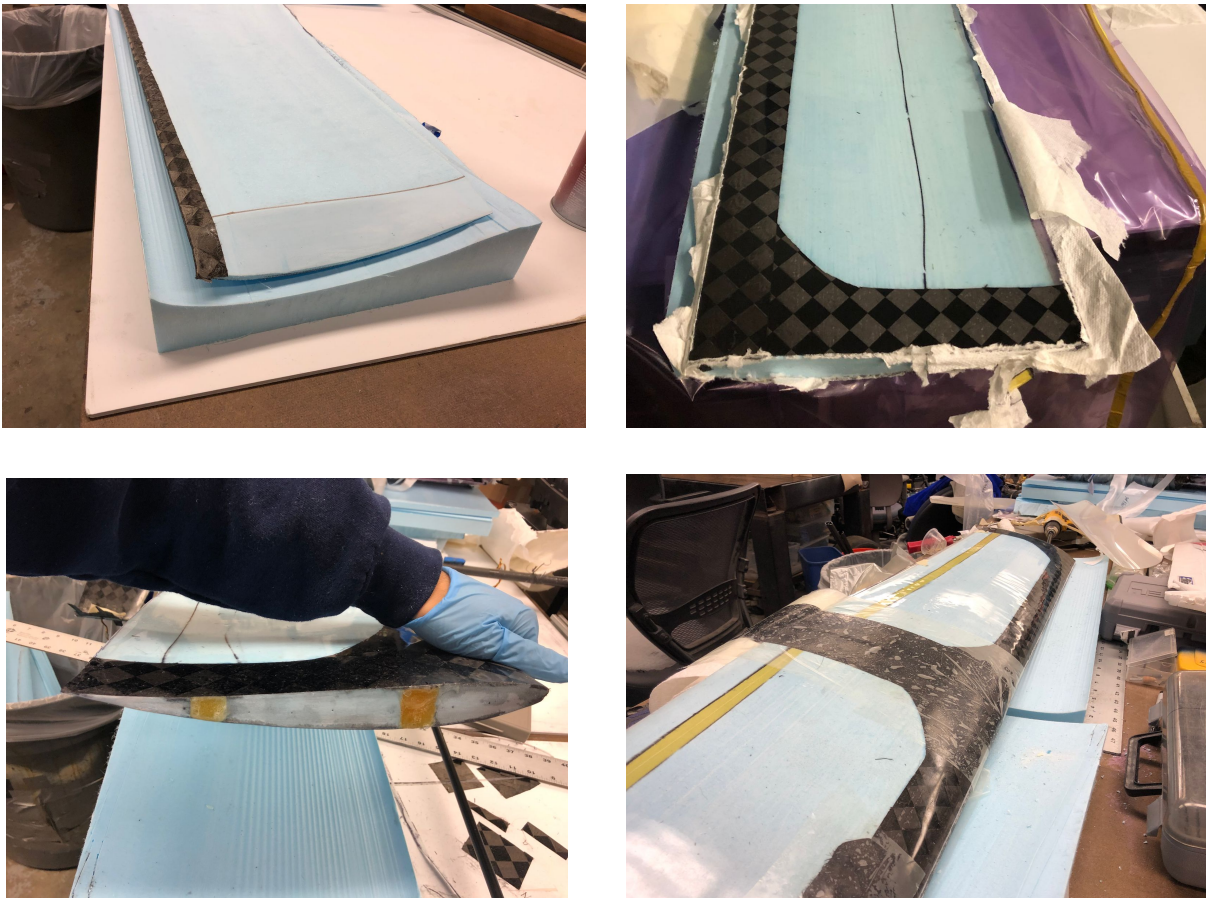


**Figure 6.2.2** Construction of the wing for the first prototype.

**Tail »** The team considered several empennage manufacturing processes, including:

- a foam-core composite process, in which the team uses a hot-wire CNC cutter to cut a tail from high-density foam and coats the structure with either composite material; or
- a balsa wood construction process, in which the team uses laser cutters to cut horizontal and vertical profiles from thin wood and covers the structures with fiberglass to strengthen the tail.

The team built and tested a prototype with a foam-core fiberglass tail, but soon found that these materials were not strong enough at high speeds; the aircraft's control horns consequently detached mid-flight. For its competition aircraft, the team decided to incorporate a foam-core carbon-fiber tail (and improve the anchoring of the control horn to the control surface).



**Other components »** The team considered wood construction and 3D printing for the fabrication of its restraint systems. Since the team preferred its relatively strong characteristics to carry loads from the heavier passengers, the team chose to build the passenger restraint system from wood. The team favored the manufacturability of 3D printing for light loads, and thus opted to build a printed luggage restraint system.

The landing gear is a custom-made aluminum build with wire tensioners. The high yield strength of aluminum allows the gear to easily absorb impacts on landing.

### 6.3 Manufacturing timeline

The team has planned to build two planes throughout the 2020 contest season. Approximately one week before beginning its fabrication process, the team implements a design freeze; sub-teams may conduct analyses and suggest changes to the plane's design at any point prior to the freeze date.

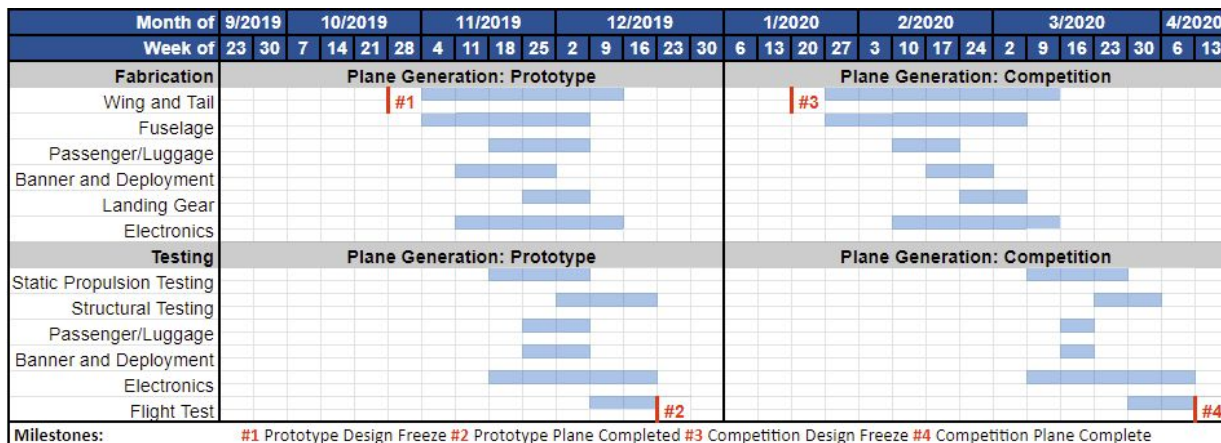


**Figure 6.3.1** Manufacturing timeline.



## 7 Testing plan

To gather flight data and optimize the performance of its competition aircraft, UCSD DBF created and executed a plan to test the aircraft's sub-systems. This section discusses the team's comprehensive testing process extensively.

### 7.1 Aircraft and sub-system testing plan

The team has planned two test flight periods throughout the 2020 competition season; this test schedule is shown in [Figure 7.1.1](#).

Month of	11/2019				12/2019				1/2020				2/2020				3/2020				4/2020				
Week of	4	11	18	25	2	9	16	23	30	6	13	20	27	3	10	17	24	2	9	16	23	30	6	13	
Testing	Plane Generation: Competition																								
Static Propulsion Testing																									
Structural Testing																									
Passenger/Luggage																									
Banner and Deployment																									
Electronics																									
Flight Test									#1																#2
Milestones:	#1 Prototype Plane Completed (12/20)												#2 Competition Plane Complete (4/10)												

[Figure 7.1.1](#) Testing schedule.

The team has conducted several tests on the aircraft's propulsion systems, structural integrity, and flight characteristics with the techniques and tools available.

**Static propulsion testing »** The team used an RC Benchmark dynamometer to measure the static thrust, rotational speed, voltage, and current of the selected propulsion system (a CM-4518/18 motor with two 14-in. diameter, 8.5-in. propellers) across various throttle settings.

**Structural integrity testing »** To verify the aircraft's structural integrity, the team performed several tests throughout the manufacturing process and prior to flight. The team first tested the carbon fiber spar for its ability to support the aircraft's full weight, then placed weights on the wings to simulate maximum loading.

After completing the final prototype, the team conducted two wingtip tests-- while unloaded and fully-loaded-- to test the integrity of the wing and fuselage joints.

### 7.2 Flight testing

To test the aircraft's flight performance in a safe manner, the team created a progressive testing plan to ensure that there was no unnecessary risk to the airframe. The plan also allows the team to find and fix



unforeseen problems and other instabilities; if any are found, the team will consult flight and telemetry data, make the changes necessary to remediate these issues, and conduct additional test flights as it sees fit.

**Pre-flight checklist »** Prior to taking off, the following conditions are checked and signatures collected:

Preflight Checklist	
Propulsions	Payload
Propeller Direction?	<input type="checkbox"/>
Propeller Secured?	<input type="checkbox"/>
Batteries Charged?	<input type="checkbox"/>
Battery Voltages +/- .3V?	<input type="checkbox"/>
Receiver Pack Charged?	<input type="checkbox"/>
Receiver On?	<input type="checkbox"/>
Connection Secured	<input type="checkbox"/>
	Weight verified? <input type="checkbox"/>
	Payload Secure? <input type="checkbox"/>
Aircraft	
	CG Verified? <input type="checkbox"/>
	Wing bolts tight? <input type="checkbox"/>
	Hatches closed? <input type="checkbox"/>
	Landing Gear Tight? <input type="checkbox"/>

**Figure 7.2.1** Pre-flight checklist.

Final Checklist	
Controls	Signatures
Receiver Connection?	<input type="checkbox"/> Pilot _____
Control Surfaces Responsive?	<input type="checkbox"/> Faculty Advisor _____
Telemetry Software On?	<input type="checkbox"/> Project Manager _____
Visual Inspection?	<input type="checkbox"/> Date _____

**Figure 7.2.2** Final checklist.

**Flight tests conducted »** The team has designated its flights using the scheme **[Flight version #] - M[Maiden flight: F, Mission #]**; a full list of test flights are listed in [Figure 7.2.3](#).

Date and location	Flight number	Mission simulated	Designation	Added weight
11 Jan 2020	1	1	1-MF	0 oz.
San Diego, California	2	1	1-M1	0 oz.
	3	2	2-MF	30 oz.
	4	2	2-M2	60 oz.
	5	2	2-M2	90 oz.
25 Jan 2020	6	3	3-MF	10 oz.
San Diego, California	7	3	3-M3	~16 oz.
	8	3	3-M3	20 oz.

**Figure 7.2.3** Table of test flights.



## 8 Performance results

UCSD DBF conducted its first tests after the prototype was completed on the week of 6 January 2020. The following section documents the results of the tests described in § 7.

### 8.1 Component and sub-system performance

The team compiled the results of the component-wise tests, and observed their performance in actual flight.

**Propulsion tests** » The team's test stand data, which gathers the propulsion system's static thrust and various electrical quantities, are documented in [Figure 8.1.1](#).

	Maximum airspeed	Maximum power	Voltage	Voltage at maximum current	Maximum current
CM-4515/18 motor 14" x 8.5" propeller	114 feet/sec.	489 W	24.5 V	23.12 V	21.15 A

[Figure 8.1.1](#) Static motor test results.

The Cobra CM-4515/18 motors are a good solution for the team's performance goals. It provided enough instant thrust to take off within 20 feet and operated efficiently while towing banners and lifting large payloads. The team encountered several easily remedied issues; unbalanced propellers created excess vibrations at certain throttle ranges and the aluminum prop-nuts unscrewed at full throttle. The plane drew 9 A of current while cruising-- a success, given the propulsion setup and size of the aircraft.

The team expected its batteries to drain quickly during takeoff-- the most intensive period of flight. This was quite evident from the team's telemetry data; short-distance takeoffs drew 60 A and used about 35 mAh from the battery pack. Overall, however, the tests confirmed the team's propulsion choices. The LiPo packs supplied enough current, did not overheat, nor excessively sag under loads in-flight.

**Structural tests** » After conducting tests at maximum load, the team inspected the spar and wing thoroughly for any visual signs of bending, yielding, or damage; there were none. Further tests, such as wingtip testing, in [Figure 8.1.2](#), were successful.



**Figure 8.1.2** Team members conducting a successful wingtip test.

The team tested the landing gear to support the entire weight of the aircraft both statically and under high impact. During one landing on rough rocks and dirt, the connection point between the landing gear and the carbon fiber boom started to weaken. The team reinforced the failure on-field, and plans to use more Kevlar twine to fully reinforce the final aircraft.

## 8.2 Complete aircraft performance

The team compiled the aircraft's extreme speeds and cruising amperage from flight telemetry data, and used frame-by-frame video analysis to estimate its takeoff distance; these values are recorded in [Figures 8.2.1](#), [8.2.2](#), and [8.2.3](#).

	Maximum airspeed	Minimum airspeed	Cruising amperage	Takeoff distance
<b>Actual 1-M1</b>	135 ft./sec.	34 ft./sec.	6.0 A	11 ft.
<b>Predicted</b>	123 ft./sec.	31 ft./sec.	5.0 A	4.9 ft.

**Figure 8.2.1** Flight performance comparison for Mission 1.

	Maximum airspeed	Minimum airspeed	Cruising amperage	Takeoff distance
<b>Actual 2-M2</b>	143 ft./sec.	51 ft./sec.	8.0 A	32 ft.
<b>Predicted</b>	127 ft./sec.	43 ft./sec.	10.0 A	21.2 ft.

**Figure 8.2.2** Flight performance comparison for Mission 2.



	Maximum airspeed	Minimum airspeed	Cruising amperage	Takeoff distance
Actual 3-M3	84 ft./sec.	41 ft./sec.	9.0 A	15 ft.
Predicted	70 ft./sec.	33 ft./sec.	19.0 A	6.6 ft.

**Figure 8.2.3** Flight performance comparison for Mission 2.

The flight data shows that the aircraft outperformed its projected top speed, but did not take off in as short a distance. Based on these results, the team will minimize the aircraft's excess drag, reduce its current draw, and increase its top speed.



**Figure 8.2.4** Take-off length documentation (~11 feet).

**Telemetry logs and data »** The raw telemetry data for **1-M1** (no-load flight) and **3-M3** (10-oz. and 16-oz. banner flight) are provided in Figures 8.2.5 through 8.2.11.

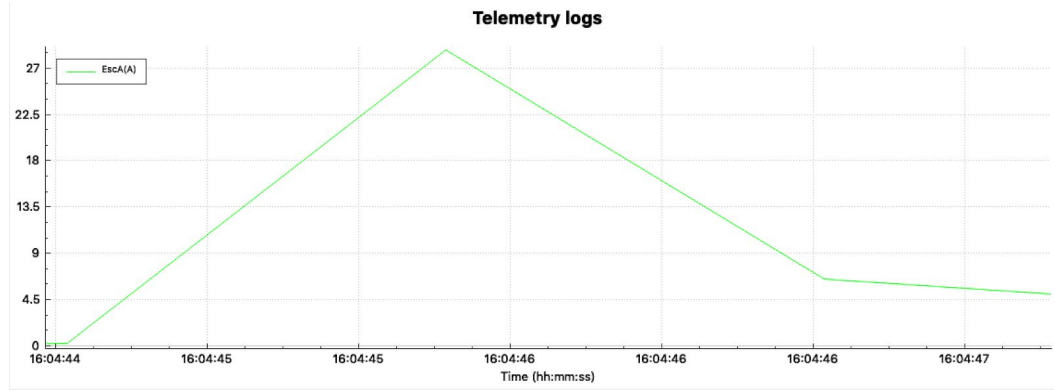


**Figure 8.2.5** ESC: amperage spike during takeoff for one motor.

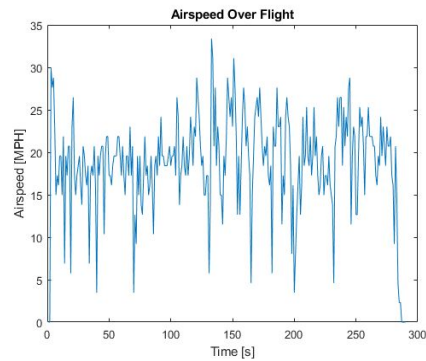


**Figure 8.2.6** Airspeed-time relationship (**1-M1**).

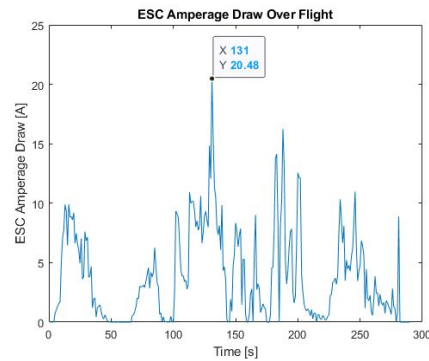


**Figure 8.2.7** ESC: Amperage draw-time relationship (**1-M1**).

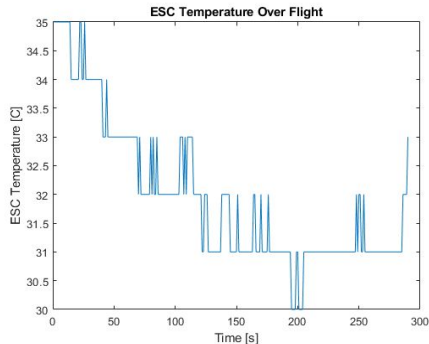


**Figure 8.2.8** ESC: Temperature-time relationship (**1-M1**).

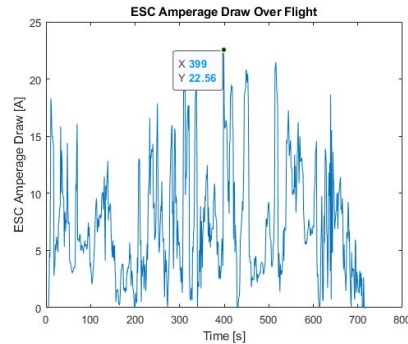


**Figure 8.2.9** ESC: Amperage draw-time relationship (**3-M3**, 10-ounce).

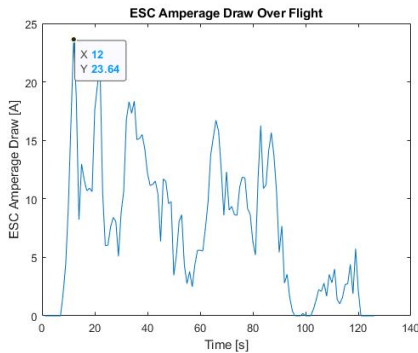


**Figure 8.2.10** ESC: Amperage draw-time relationship (**3-M3**, 16-ounce).

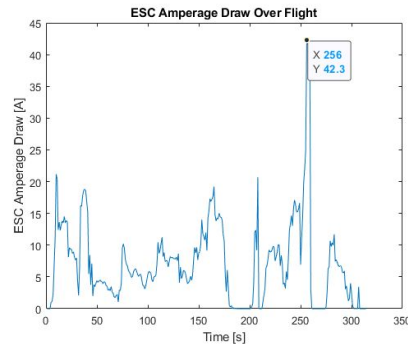


**Figure 8.2.11** ESC: Amperage draw-time relationship (full throttle).

Figures 8.2.6 through 8.2.8 show the telemetry data for a standard flight without payload or banners; ESC temperatures stayed well under their safety rating, while current draw and amperage stayed within a reasonable range. Figures 8.2.9 through 8.2.11 compares the amperage draw across different banner sizes and throttle percentages. As the team increased banner sizes, the aircraft observed a slight increase in amperage; the aircraft and propulsion system performed quite efficiently under extra loads. The emphasized point in Figure 8.2.11 shows the approximate maximum current draw.

**Future work »** The team plans to make several modifications to, and conduct several tests of, the final aircraft to improve aircraft performance. The fuselage will be analyzed in order to lighten the weight and carry more passengers if possible. Wiring will be run internally to reduce parasitic drag and the fuselage will be modified to blend into the wing. Minor adjustments to battery size will occur if the team finds a need to change the flying style or if weight could be saved reducing battery capacity for certain missions. The banner material will be experimented on to reduce fluttering and excess drag. During this time, many successive test flights will occur in order for practice to be given to the pilot and crew. By competition, the team hopes to have a well-tested aircraft that is optimized for both high performance and high reliability.



## 9 Bibliography

- [1] Nicolai, L. M. and Carichner, G. E., "Propeller propulsion systems," *Fundamentals of Aircraft and Airship Design*, 2<sup>nd</sup> ed., Vol. 1, AIAA, Reston, VA, 2010.
- [2] Nicolai, L. M., *Fundamentals of Aircraft Design*, 1<sup>st</sup> ed., METS Inc., Xenia, OH, 1975.
- [3] Yehout, T. R., *Introduction to Aircraft Flight Mechanics: Performance, Static Stability, Dynamic Stability, and Classical Feedback Control*, AIAA, Reston, VA, 2003.
- [4] Anderson, J. D., *Fundamentals of Aerodynamics*, 4<sup>th</sup> ed., McGraw Hill, Boston, MA, 2007.